



Angiopoietin-2-induced lymphatic endothelial cell migration drives lymphangiogenesis via the β 1 integrin-RhoA-formin axis

Racheal Grace Akwii¹ · Md. Sanaullah Sajib¹ · Fatema Tuz Zahra¹ · Paul Tullar² · Masoud Zabet-Moghaddam³ · Yi Zheng⁴ · J. Silvio Gutkind⁵ · Colleen L. Doci⁶ · Constantinos M. Mikelis^{1,7} 

Received: 2 April 2021 / Accepted: 8 November 2021 / Published online: 1 February 2022
© The Author(s), under exclusive licence to Springer Nature B.V. 2022

Abstract

Lymphangiogenesis is an essential physiological process but also a determining factor in vascular-related pathological conditions. Angiopoietin-2 (Ang2) plays an important role in lymphatic vascular development and function and its upregulation has been reported in several vascular-related diseases, including cancer. Given the established role of the small GTPase RhoA on cytoskeleton-dependent endothelial functions, we investigated the relationship between RhoA and Ang2-induced cellular activities. This study shows that Ang2-driven human dermal lymphatic endothelial cell migration depends on RhoA. We demonstrate that Ang2-induced migration is independent of the Tie receptors, but dependent on β 1 integrin-mediated RhoA activation with knockdown, pharmacological approaches, and protein sequencing experiments. Although the key proteins downstream of RhoA, Rho kinase (ROCK) and myosin light chain, were activated, blockade of ROCK did not abrogate the Ang2-driven migratory effect. However, formins, an alternative target of RhoA, were identified as key players, and especially FHOD1. The Ang2-RhoA relationship was explored in vivo, where lymphatic endothelial RhoA deficiency blocked Ang2-induced lymphangiogenesis, highlighting RhoA as an important target for anti-lymphangiogenic treatments.

Keywords Angiopoietin-2 · Ang2 · RhoA · Integrins · Formins · Lymphangiogenesis · HDLEC · Lymphatic endothelial cells · Small GTPase · Cell migration

Introduction

The Ang-Tie system comprises of the endothelial Tie1 and Tie2 (Tek) receptor tyrosine kinases (RTK) and the angiopoietin (Ang) growth factor ligands of the Tie2 receptor: Ang1, Ang2 and Ang4 [1–4].

Ang1 rapidly auto-phosphorylates the Tie2 receptor but does not directly promote the growth of cultured endothelial cells [5, 6], while Ang2 mainly inhibits Ang1-induced Tie2 phosphorylation [2]. Although an initial antagonistic role was attributed to Ang2, later studies demonstrated that Ang2 could also phosphorylate Tie2, though not to the same extent as Ang1, and thus induce endothelial cell functions [7, 8]. High concentrations of Ang2 were shown to induce blood endothelial cell (BEC) survival through phosphoinositide 3-kinase (PI3K) and Akt activation [9]. Due to these contradicting functions, the role of Ang2 is considered context-dependent. Tie1, the other receptor of the Ang/Tie pathway, has been shown to regulate this context-dependent role of Ang2 [10].

✉ Constantinos M. Mikelis
constantinos.mikelis@ttuhsc.edu

¹ Department of Pharmaceutical Sciences, School of Pharmacy, Texas Tech University Health Sciences Center, 1406 S. Coulter St., Amarillo, TX 79106, USA

² Department of Obstetrics and Gynecology, School of Medicine, Texas Tech University Health Sciences Center, Amarillo, TX 79106, USA

³ Center for Biotechnology and Genomics, Texas Tech University, Lubbock, TX 79409, USA

⁴ Center and Blood Diseases Institute, Cincinnati Children's Hospital Medical Center, University of Cincinnati College of Medicine, Cincinnati, OH 45229, USA

⁵ Department of Pharmacology, UCSD, San Diego, CA 92093, USA

⁶ Program in Exercise and Sport Science, College of Health Professions, Marian University Indianapolis, Indianapolis, IN 46222, USA

⁷ Department of Pharmacy, University of Patras, Patra 26504, Greece

The participation of Ang2 in angiogenesis and lymphangiogenesis is established, and its effect on endothelial cell functions is known to be inhibitory [2, 8, 11] or stimulatory [7–9, 12, 13] under certain conditions, such as specific cell types, high concentrations, inflammation, and related pathophysiological conditions. Although during physiological angiogenesis Ang2 acts as an antagonist in BECs [2], in lymphangiogenesis, its role seems to be more agonistic than antagonistic. In lymphatic endothelial cells (LECs), high dose treatment of Ang2 phosphorylated the Tie2 receptor and promoted LEC proliferation and cell survival [13]. The angiogenic and anti-apoptotic activity of Ang2, through binding to the Tie2 receptor and activation of the downstream Tie2/Akt signaling pathway, has been attributed to limited physical association of Tie2 with Tie1, due to the decreased Tie1 expression in the LECs compared to BECs, implying an inhibitory effect of Tie1 on Ang2-induced Tie2 activation in LECs [14].

The Tie receptor is encoded by the Tek gene, whose expression can be detected in early embryonic development. The Tie receptor genes (*Tie1* and *Tie2*) are expressed in the embryonic endothelium thereafter [15, 16]. During vasculogenesis and early angiogenesis, the expression of the Tie receptors follows the expression of the VEGF receptors (VEGFRs: VEGFR1 and VEGFR2) [16, 17], with the VEGFR beginning earlier, at embryonic day 7.0 (E7.0) [17–19], and the Tie2 expression being detected at E8.0 in the flk-1-expressing mesoderm, signifying a role of the Tek receptors during subsequent vascularization of the embryo [15, 16, 20–22]. Tie2 expression has been detected in the lymphatic endothelial cells during embryonic lymphangiogenesis as well as in adulthood. Tie2 was detected in LECs isolated from E11, E13 and E15 embryos by FACs analysis [23]. In the adult mice, staining with anti-Tie2 antibody of the intestinal lymphatic vessels revealed the expression of Tie2 in the lacteal lymphatics, though its expression was significantly weaker in the LECs than in the BECs [23]. In a similar pattern, Tie2 expression was detected in the adult mouse ear lymphatic endothelium, although it was weaker compared to the blood vascular endothelium [24]. On the other hand, some studies have demonstrated that during embryogenesis Tie2 is not expressed in the lymphatics, since no *Tie2* expression was detected in E11.5, E13.5 and E15.5 *Tie2-GFP* mouse embryos and *Tie2-lacZ* did not label LECs emerging from the cardinal vein at E13.5–14.5 [25]. Via the same *Tie2-GFP* model it was assessed that dermal lymphatic vessels do not express Tie2 at E14.5 and E16.5 [26], maintaining the question regarding Tie2 expression in the lymphatics.

Ang2 is expressed in the endothelium, macrophages, muscle cells and tumor cells [2, 9, 27, 28]. Ang2 expression in the quiescent endothelium is limited, but it is induced upon endothelial stimulation in diseased and angiogenic

conditions, such as tumors [29–33]. It is stored in the Weibel–Palade bodies and released by the endothelial cells upon stimulation [34]. Ang2 induces activity of the endothelial cells via an autocrine manner: phorbol 12-myristate 13-acetate (PMA), thrombin, or histamine (in certain endothelial cell types) lead to Ang2 secretion [34]. PMA treatment of co-culture spheroids of endothelial and smooth muscle cells led to a rapid disintegration of the surface endothelial cell monolayer, evidenced by massive detachment of endothelial cells. This was abrogated upon Ang2 silencing, signifying that endothelial cell-derived Ang2 release was responsible for the disturbed monolayer [34]. Ang2 release by stressed endothelial cells is regulated in a FOXO1-dependent manner, as FOXO1 knockdown inhibited wortmannin-induced Ang2 release [35]. This FOXO1-mediated effect on Ang2 levels upon Tie1 inhibition in inflammation was further demonstrated in a *Mycoplasma pulmonis* infection model [10], further supporting its autocrine effect. The outcome of Ang2 paracrine effect on different cell types depends on Tie2 and integrin expression [36]. This chemotactic behavior of Ang2 has been demonstrated on endothelial cells, which tend to migrate towards an increasing concentration of exogenous Ang2 [7, 9, 13, 36]. Similar chemotactic effect was also observed in non-endothelial cells: RAW 264.7 murine macrophage cells [37] and neutrophils [38] migrate towards an increasing Ang2 concentration.

The expression of Ang2 is highly regulated. In adults under physiological conditions, it is mainly expressed in vascular remodeling sites, particularly the ovary, placenta and uterus [2]. Ang2 expression is also triggered by inflammatory mediators, such as thrombin [30] and estrogen [39] and hypoxic conditions [40]. In inflammatory conditions and cancer Ang2 is considered a modulator of tumor angiogenesis and metastasis and has been proposed as a biomarker, by several studies that have reported a correlation between elevated levels of Ang2 and disease progression [3].

The small GTPase RhoA is a principal mediator of actomyosin structure and dynamics, regulating cellular functions, such as cell migration and retraction [41, 42] and in endothelial cells plays an important role in vascular functions controlling angiogenesis and vascular permeability [43]. RhoA is required for VEGF-induced endothelial cell migration and angiogenesis, as inhibition of RhoA or its downstream signaling blocks VEGF-induced angiogenesis in vitro [44–47]. Simultaneously, it participates in the downstream signaling cascades of diverse angiogenesis mediators, such as Sphingosine-1-phosphate (S1P) [47], providing a common target for angiogenesis inhibition. The molecular mechanisms of lymphangiogenesis are focused mainly on VEGF-C and VEGF-D, a sub-family of the VEGF growth factors and their corresponding receptor VEGFR-3 [48–50]. RhoA is activated by VEGF-C in endothelial and cancer

cells and its inhibition blocks VEGF-C-induced angiogenesis and cancer metastasis respectively [51, 52].

Although its role in disease has been mildly overlooked, lymphangiogenesis is a vital process in disease pathology. Breast cancer depends on the lymph nodes for metastasis [53]. The presence of cancer cells in the lymph nodes is a strong predictor of recurrence and survival in breast cancer patients. Micrometastases in the lymph nodes act as homing signals for distant organ metastasis and are considered to occur before most primary tumors are clinically detectable [54], making histological staining of lymph nodes and lymph node staging of tumors vital in proper diagnosis and treatment [54, 55]. Apart from cancer, lymphangiogenesis inhibition could be beneficial in certain pathologies. In Milroy disease, a form of primary lymphedema, skin biopsies of patients' swollen feet revealed the presence of abundant lymphatic vessels, suggesting a more complex mechanism of lymphatic failure [56, 57]. Kaposiform Lymphangiomatosis, another rare condition affecting the lymphatic system, is characterized by expansion and interconnection of the lymphatic vessels [58, 59], highlighting the role of the lymphatic system in disease pathology and strengthening the need to further understand the molecular regulation of this system.

The role of the RhoA/ROCK pathway in the lymphatic system is not unknown. ROCK inhibition in LECs mimicked VEGFR2 inhibition, leading to straighter junctions in vitro and increased lacteal junction zippering in vivo, thus reducing the chylomicrons presence in the lacteal lumen [59]. Pre-treatment of HDLEC with the ROCK inhibitor Y-27632 inhibited the junctional reduction of CLDN5 upon EphrinB2 blockade and an opposite effect was observed with Rac1 [60]. ROCK inhibition ameliorated the FOXC1,2 double knockdown-induced actin filamentation, a phenomenon that affects the formation of postnatal lymphatic valve maturation and maintenance [61].

Given that Ang2 is considered a lymphangiogenesis mediator, the aim of this study was to investigate whether RhoA is a downstream target of Ang2, if it is required for Ang2-mediated functions and to delineate the signaling pathway involved. We illustrate that Ang2 treatment activates RhoA in both human dermal lymphatic endothelial cells (HDLEC) and human umbilical vein endothelial cells (HUVEC), but induces angiogenesis, assessed by cell proliferation and migration specifically in HDLECs. Inhibition of RhoA using C3 toxin or knockdown by siRNAs potently abrogated Ang2-induced cell migration. The Ang2-driven effect was independent of both Tie1 and Tie2 expression, but required β 1 integrin, a binding partner of Tie2 and Ang2. Although the downstream ROCK/pLMC pathway was activated by Ang2 stimulation, ROCK inhibition did not abolish the HDLEC migration. Instead, blockade of formins, alternative downstream RhoA targets, inhibited the migration of the LECs. In vivo, Ang2 induced lymphangiogenesis in the ear

sponge assay. Furthermore, lymphatic endothelial-specific RhoA deficiency hindered Ang2-driven lymphangiogenesis. Together, this highlights lymphatic endothelial RhoA as a target for blockade of Ang2-induced lymphangiogenesis for translational intervention.

Methods

Cell culture

The human dermal lymphatic endothelial cells (HDLEC) used in this study were obtained from PromoCell (Cat# C-12216). For the cell culture optimization of the HDLEC, endothelial cell growth media from different companies were tested and the HDLEC were finally cultured with endothelial cell growth base medium (Cat# CCM027) from R&D Systems with its corresponding endothelial cell growth supplement (Cat# CCM027). HDLEC were plated on collagen-coated (10 μ g/ml) dishes. HUVEC were isolated from human umbilical cords under the Texas Tech University Health Sciences Center Institutional Review Board-(IRB)-approved protocol A15-3891, and informed consent was obtained from all donors [47, 53, 62]. HUVEC were cultured in M199 medium (Corning, Cat# MT10060CV), supplemented with 15% Fetal Bovine Serum (FBS) (GIBCO™, Cat# 10438026), 150 μ g/ml Endothelial Cell Growth Supplement (ECGS), 5 U/ml heparin sodium and 1 \times Antibiotic–Antimycotic solution (GIBCO™, Cat# 15240-062) (EC complete medium) [47, 63, 64]. HUVEC were plated on 1% gelatin-coated dishes. Each batch of primary endothelial cells was derived from a single donor and the cells of at least two donors were used in the experiments to ensure reproducibility. Both HUVEC and HDLEC were used between passages 1 and 6 and cell cultures were maintained at 37 °C and 5% CO₂.

Mice

Animal studies were carried out according to TTUHSC IACUC-approved protocols, in compliance with the Guide for the Care and Use of Laboratory Animals. Mice were maintained on a C57BL/6 background and both males and females were used for experiments. The generation of the *RhoA^{fl/fl}*; *Tom-GFP^{fl/fl}* mice has been described previously [65]. Conditionally-regulated endothelial-specific RhoA deficient mice were obtained by crossing the *RhoA^{fl/fl}*; *Tom-GFP^{fl/fl}* mice with mice carrying a Cre-mediated recombination system, driven by the *Prox1* promoter (*Prox1-CreERT²*) [25]. 2 mg/mouse/day of Tamoxifen, dissolved in Miglyol™, were intraperitoneally (i.p.) injected for 5 consecutive days and ear sponges were implanted a week later. Genotyping of the *RhoA^{fl/fl}*; *Tom-GFP^{fl/fl}*; *Prox1-CreERT²* mice was

performed by Touchdown polymerase chain reaction (PCR) on mouse genomic DNA extracted by tail biopsies. PCR was performed with the JumpStart REDTaq ReadyMix Reaction Mix (Millipore Sigma; Cat# P0982). Littermates were used as controls in all experiments.

Mouse dermal lymphatic endothelial cell isolation

A week after tamoxifen treatment, the mice were humanely euthanized, the skin of the torso was removed, cut in pieces and digested in Dispase (Life Technologies, Cat# 17105-041; 2 mg/ml in serum free medium) overnight with mild agitation at 4 °C. Dermis was separated from the epidermis and dermis was transferred, minced into 1–2 mm² pieces and digested with Collagenase Type II (Life Technologies, Cat# 17101-015; 2 mg/ml in DMEM 0.1% BSA) at 37 °C for 2 h with occasional agitation. The cell suspension was filtered through a 70 µm cell strainer, centrifuged at 1500 rpm for 5 min and plated on collagen-coated dishes (day 0) in complete LEC media. Media was replaced with endothelial cell complete media after two PBS washes, every day until day 4. For purification, sheep anti-rat IgG Dynabeads (Invitrogen) were incubated with anti-mouse LYVE-1 mAb (ReliaTech, Cat# 103-PA50; 22.5 µl Ab per 150 µl dynabead solution) overnight at 4 °C and washed three times with PBS supplemented with 0.1% BSA and 2 mM EDTA, using a magnetic separator. On day 5, the first purification was performed by incubating cells with the pre-coated beads for 10 min at RT under continuous agitation. Cells were then washed with PBS twice, followed by trypsinization. The cells were recovered with a magnetic separator, washed four times, resuspended in full media, and cultured in collagen-coated plates. The potential contamination of the lymphatic dermal endothelial cells with other Lyve-1-expressing cells, such as macrophages, was identified by performing Flow cytometry for Lyve-1 and F4/80 (BioLegend, Cat# 123107), where less than 10% of macrophage contamination was verified (not shown). Cells were then processed for immunoblot analysis.

siRNA transfection

For gene knockdown experiments, cells were transfected with 50 nM of two siRNA sequences for RhoA (RhoA#1; ID: s758 and RhoA#2; ID: s759), two siRNA sequences for Tie1 (Tie1#1; ID: s14141 and Tie1#2; ID: s14142), two siRNA sequences for Tie2 (Tie2#1; ID: s13983 and Tie2#2; ID: s13984), siRNA sequence for integrin subunit β1 (ID: s7575) or noncoding siRNA (Cat# 4390844), all from Life Technologies. The siRNA sequences for FHOD1 (Gene ID: 29109; Cat# M-013709-01) and mDia1 (Gene ID: 1729; Cat# M-010347-02) were from Dharmacon. DharmaFECT 1 (Dharmacon, Cat# T-2001-02) transfection reagent was used for transfection, according to the manufacturer's instructions.

Briefly, the cells were cultured in 6-wells to 80% confluency, then transfected with siRNA using Dharmafect in starvation medium. Using two sets of microcentrifuge tubes, in the one set the siRNAs were diluted to a concentration of 100 nM in 200 µl of antibiotic- and serum-free medium (starvation medium) and in the other set Dharmafect was diluted to 20× in 200 µl of starvation medium and tubes were vortexed for 5 s. After vortexing, the tubes were left to stand for 5 min at room temperature (RT). The diluted siRNAs were then transferred to their corresponding tubes containing Dharmafect and the tubes were again vortexed for 5 s each, briefly spun down and left to stand for 20 min at RT. Meanwhile, the wells of the 6-well plate were rinsed with PBS to remove FBS and 1600 µl of starvation medium was pipetted into each well. 400 µl of the combined siRNA and Dharmafect solution was then pipetted into the corresponding wells and incubated for 6 h at 37 °C in 5% CO₂. After the 6-h incubation period, the medium was replaced with full medium and cells were incubated for 36 h more. All experiments were performed 48-h post-transfection.

RhoA pulldown assay

RhoA activity was assessed, as previously reported [42, 43, 47] using GST-Rhotekin conjugated with Glutathione Sepharose 4B beads (GE Healthcare Life Sciences, Cat# 45-000-139). The GST-RBD plasmid was a gift from Martin Schwartz (Addgene plasmid# 15247) [66]. Briefly, confluent 6-well plates were starved for 6 h, then stimulated with Ang2 for 3 min or as indicated in the time-course experiments. Cells were lysed using RhoA lysis buffer [20 mM HEPES, pH 7.4, 0.1 M NaCl, 1% Triton X-100, 10 mM EGTA, 40 mM β-glycerophosphate, 20 mM MgCl₂, 1 mM Na₃VO₄, 1 mM dithiothreitol (DTT), 10 µg/ml Aprotinin, 10 µg/ml Leupeptin and 1 mM phenylmethylsulfonyl fluoride (PMSF)], centrifuged and incubated with GST-Rhotekin immobilized on Glutathione Sepharose beads for 30 min at 4 °C. The beads were washed three times with lysis buffer and eluted in 2×Laemmli sample buffer. Equal volumes of cell lysate were used to assess total RhoA. Associated GTP-bound forms of RhoA were released with SDS–polyacrylamide gel electrophoresis loading buffer and analyzed by western blot analysis using a monoclonal antibody against RhoA, as described below.

Immunoprecipitation

Immunoprecipitation was performed as previously described [63, 67]. Briefly, cells were lysed using RIPA buffer, centrifuged at 13,000 × g for 5 min at 4 °C. As a pre-clearing step, 5 µl of Dynabeads protein A (Invitrogen, Cat# 10002D) and 5 µl of Dynabeads protein G (Invitrogen, Cat# 10004D) were mixed, washed with RIPA buffer, and were incubated

with the supernatant for 10 min at 4 °C under continuous agitation. The samples were centrifuged at 1000 × *g* for 5 min at 4 °C and the supernatant was processed for immunoprecipitation, as following: equal volumes of pre-cleared supernatant were mixed with the 10 µl of the antibody and incubated overnight at 4 °C under continuous agitation. 10 µl of Dynabeads protein A and 10 µl of Dynabeads protein G were mixed, washed and resuspended in 100 µl RIPA buffer, added to the samples and incubated for 2 h at 4 °C under continuous agitation. The samples were centrifuged at 1000 × *g* for 5 min at 4 °C, the supernatant was discarded, and the beads rinsed three times in RIPA buffer using a Dynal magnet. 40 µl of 2× sample buffer were added, tubes were heated at 95–100 °C for 5 min and centrifuged at maximum speed for 5 min. Samples were then destined for SDS-PAGE and either stained using Coomassie blue dye or immunoblotted, as described below.

Coomassie blue staining

The gel was rinsed in dH₂O and fixed in destaining solution (45% methanol, 10% acetic acid and 45% dH₂O) for 1 h. The gel was rinsed three times, for 5 min each and stained with filtered Coomassie blue staining solution (0.25% Coomassie Blue R-250 (Fisher, Cat# BP101) in 45% methanol, 10% acetic acid and 45% dH₂O) for 3 h. The gel was rinsed three times, for 5 min each and destained using the destaining solution overnight at 4 °C, followed by 3 rinses, 5 min each and stored in 1% acetic acid for further processing.

Immunoblotting

Immunoblot analysis was performed as previously described [47, 68]. The cells were lysed on ice in RIPA buffer (10 mM Tris–HCl, 1 mM EDTA, 0.5 mM EGTA, 1% Triton X-100, 0.1% sodium deoxycholate (SDS), 0.1% SDS and 140 mM NaCl), supplemented with protease and phosphatase inhibitors (Halt Protease and Phosphatase Inhibitor Cocktail, Thermo Scientific, Cat# 78445), unless specified. Cell lysates were centrifuged at 12,000 × *g* for 5 min at 4 °C. Samples were eluted in Laemmli sample buffer, heated at 95–100 °C and centrifuged at maximum speed for 5 min. Samples were run on SDS-PAGE gel at 110 V and transferred on an Immobilon P, polyvinylidene difluoride membrane (Millipore Sigma, Cat# IPVH304F0). The membrane was blocked using 5% milk in TBS-Tween (TBS-T), probed with primary antibodies for RhoA (Cell Signaling Technology, Cat# 2117S.), Tie1 (Cell Signaling Technology, Cat# 23111S), Tie2 (R&D Systems, Cat# AF313), integrin β1 (Cell Signaling Technology, Cat# 34971), mDial1 (Cell Signaling Technology, Cat# 5486), FHOD1 (ECM Biosciences, Cat# FM3521), Ang2 (Cell Signaling Technology, Cat# 2948), Ang2 (Santa Cruz Biotechnology, Cat#

sc-74403) or β-actin (Cell Signaling Technology, Cat# 3700S), GEF-H1 (Cell Signaling Technology, Cat# 4076), PDZ-RhoGEF (Abcam, Cat# ab110059), LARG (Abcam, Cat# ab136072), β-tubulin (Cell Signaling Technology, Cat# 2146), PY—4G10 (Millipore, Cat# 05-1050X), Mouse IgG (Santa Cruz Biotechnology, Cat# sc-2025) and secondary anti-rabbit (Cat# 4010-05), anti-mouse (Cat# 1010-05), and anti-goat (Cat# 6420-05) horseradish peroxidase-(HRP)-conjugated antibodies (all from Southern Biotech). Immunoreactive bands were visualized using Immobilon Western Chemiluminescent HRP substrate (Millipore Sigma, Cat# WBKLS0500). Band intensity was quantified using the ImageJ image analysis software (National Institutes of Health).

Cell migration assay

Cell migration was performed as previously described [42, 47]. Briefly, a 48-well Boyden chamber with 8-µm pore size polyvinyl pyrrolidone-free polycarbonate membrane (NeuroProbe, Cat# PFB8) pre-coated with collagen (10 µg/ml) was used. Confluent cells were starved for 4 h or treated in starvation medium, trypsinized using Trypsin–EDTA and centrifuged. The cells were then resuspended in starvation medium and counted using the haemocytometer counting chamber. 50,000 cells in 50 µl of starvation medium were added in each well of the upper compartment of the chamber with starvation medium (control) or agent (treatment) in the lower compartment of the corresponding wells and were incubated for 6 h at 37 °C with 5% CO₂. The membrane was fixed in methanol for 10 min, stained with hematoxylin for 40 min at RT, washed with dH₂O, and then stretched on a glass slide with lower side facing down and all cells on the top (non-migrating) were carefully removed. Migrated cells (lower side) were counted using a brightfield microscope (Microscoptics, IV-900) at 40× magnification. Number of cells was quantified in a blinded manner.

Tube formation assay

Matrigel tube formation assay was performed as previously described [64, 69]. 40 µl/well of RGF-Basement Membrane Extract (Trevigen, Cat# 3433) were pipetted in wells of a 96-well plate and left to polymerize for 20 min at 37 °C with 5% CO₂. Cells were resuspended in starvation medium and counted. 10,000 cells were added per well in the presence/absence of Ang2 and incubated for 6 h at 37 °C with 5% CO₂. Images of sprouts were captured using a bright-field microscope (Microscoptics, IV-900) connected with a digital camera (AmScope FMA050) at 4× magnification and later analyzed for number of nodes, number of junctions and total sprout length using the “Angiogenesis analyzer” [70] plug-in

in ImageJ image analysis software (National Institutes of Health).

Cell proliferation and toxicity assay

Cell proliferation was evaluated through the MTT (3-[4,5-dimethylthiazol-2-yl]-2,5-dimethyltetrazolium bromide) (Fisher, Cat# AC15899) colorimetric assay, as previously described [47]. 500 μ l of complete media containing 20,000 cells were pipetted per well of a 24-well plate and incubated for 24 h at 37 °C under 5% CO₂. Then, cells were starved overnight and treated with Ang2 for 24 h. At the end of the incubation period MTT stock solution (5 mg/ml) was added (50 μ l/well) for 2 h to allow for formazan crystal formation. Then, medium was removed, cells were washed with PBS pH 7.4 and formazan crystals were dissolved with 150 μ l acidified isopropanol (0.33 ml HCl in 100 ml isopropanol) upon agitation. 100 μ l of the solution were transferred to a 96-well plate, where absorbance values were obtained using a microplate reader at 570 nm. For cytotoxicity experiments, the cells were pretreated with the agent for the desired time and then treated with MTT, following the same protocol.

RNA isolation and qRT-PCR analysis

RNA isolation was performed using the Qiagen's RNeasy Mini Kit (Qiagen, Cat#: 74104) following the manufacturer's instructions. mRNA purity and concentration were determined using the NanoDrop Lite Spectrophotometer (Thermo Scientific). mRNA was transcribed to cDNA using Verso cDNA synthesis kit (Thermo Scientific, Cat#: AB-14531/A), following the manufacturer's instructions. Subsequent qRT-PCR was performed using SYBR Green PCR MasterMix (Applied biosystems by Thermo Fisher Scientific, Cat#: 4309155) in a Bio-Rad CFX96 Real-Time PCR machine. Gene expression levels of the genes of interest were normalized with β -actin gene expression and the $\Delta\Delta$ CT method was used for three replicates from each experiment.

In-gel digestion for LC–MS/MS

The distinct protein bands on SDS-PAGE were isolated and in-gel digestion was performed as previously described [71]. In brief, the gel isolates were washed with a 1:1 mixture of ACN/100 mM NH₄HCO₃ twice for 10 min to destain the gels. Reduction was performed by adding 100 μ l of 10 mM dithiothreitol (DTT) solution for 1 h at 56 °C. After reduction, the spots were alkylated by adding 50 μ l of iodoacetamide solution (55 mM in 40 mM NH₄HCO₃) and incubating in the dark for 30 min. The gel isolates were washed once more with ACN/100 mM NH₄HCO₃ and dehydrated by adding 100% ACN and air-dried. The digestion took place with 30 μ l of trypsin solution (12.5 ng/ μ l in 25 mM NH₄HCO₃)

overnight at 37 °C. Peptide extraction was performed twice using 1:1 mix of ACN/water, 0.1% formic acid solution. The extracted peptide solutions were dried in the speed vacuum centrifuge and the peptides were resuspended in 10 μ l of 0.1% formic acid for nano-LC–MS/MS analysis.

LC–MS/MS

A Dionex 3000 Ultimate nano-LC (Dionex, Sunnyvale, CA) interfaced to a Q-Exactive HF mass spectrometer (Thermo Scientific) that is equipped with EASY-Spray™ source was used for the analysis. Tryptic digests were first loaded to an Acclaim PepMap100 C18 guard column (3 μ m, 100 Å, Dionex) at a flow rate of 3 μ l/min for on-line desalting. Next, the separation of peptides was achieved using an Acclaim PepMap100 C18 capillary column (75 μ m ID \times 150 mm, 2 μ m, 100 Å, Dionex) at 0.3 μ l/min in 120 min. The mobile phase A contained 2% ACN, 0.1% FA and 98% water, while mobile phase B contained 0.1% formic acid in 98% ACN with 2% H₂O. The LC gradient was the following: Solvent B was kept at 5% for the first 10 min, increased from 5 to 20% over 55 min, 20–30% over 25 min, 30–50% over 20 min, 50–80% over 1 min, kept at 80% for 4 min, decreased from 80 to 5% over 1 min and finally maintained at 5% over 4 min. The Q-Exactive HF was used in data dependent acquisition mode. The scan events were set as a full MS scan of m/z 400–2000 at a mass resolution of 60,000, followed by HCD MS/MS scan repeated on the 20 most intense ions selected from the previous full MS scan with an isolation window of m/z 2.0. The normalized collision energy was set to 35%. The dynamic exclusion was enabled with repeat count of 2, repeat duration of 30 s and exclusion duration of 90 s. Data were analyzed by the Proteome Discoverer version 2.2 and MASCOT version 2.6.

Ear sponge assay

The ear sponge assay was performed as previously described [72]. Briefly, 3 mm ear sponges were prepared using a biopsy punch and incubated with 20 μ l of starvation medium with or without Ang2 (50 ng/ml) for 30 min at 37 °C. Sponges were briefly immersed 3 times in a collagen mix solution (0.1% acetic acid: collagen type I stock solution (Corning, Cat# 354249): FBS- and antibiotic-free phenol-red containing medium at a 4:4:1 ratio) and incubated for 30 min at 37 °C, all in aseptic conditions. Mice were anesthetized and the sponges were implanted into the mouse ears for either 14 or 21 days. At the end of the implantation period, mice were euthanized, and ear sponges removed, cryosectioned and immunofluorescence staining was performed.

Immunofluorescence staining

Ear sponge sections

Tissue immunostaining was performed on 10 μm -thick ear sponge cryosections. Briefly, the sections were fixed with 4% PFA for 20 min at RT. After two washes with PBS, the sections were incubated with 0.2% Triton X-100 in PBS for 10 min at RT, followed by two 5-min PBS washes. The sections were blocked with 3% BSA in PBS for 2 h at RT and incubated with 10 $\mu\text{g}/\text{ml}$ goat anti-mouse LYVE1 antibody (R&D Systems, Cat# AF2125) and 1:500 rat anti-mouse, PE-conjugated CD202b (TIE2) antibody (Invitrogen, Cat# 12598782) in 3% BSA overnight at 4 °C. The sections were washed with two 10-min PBS washes and incubated with donkey anti-goat Alexa 488 secondary antibody (Invitrogen, Cat# A-11055), in 1:500 dilution in 3% BSA in PBS for 2 h in the dark at RT. The sections were washed with two 10-min washes with PBS. Nuclear staining was performed with Hoechst 1:2000 in PBS for 10 min at RT in the dark. After two more brief and two 10-min washes with PBS, the sections were mounted, incubated for 2 h in the dark at RT and then stored at 4 °C in the dark till imaging (below).

Cell monolayers

For phalloidin staining, cells were cultured on Collagen I-treated cover glasses (22 \times 22) in a 6-well plate. At > 70% confluency, the cells were treated or stimulated as indicated and rinsed in ice cold PBS. The cells were fixed with 4% PFA in PBS for 10 min at RT. After two 5-min washes with PBS, the cells were incubated with 0.2% Triton X-100 in PBS for 10 min at RT, followed by two 5-min washes with PBS. After blocking with 3% BSA in PBS for 1 h at RT they were incubated with 1:1000 Alexa 594 Phalloidin (Molecular Probes, Cat# A12381) with 3% BSA in PBS for 20 min at RT. For experiments for junctional proteins the slides were incubated with primary antibodies for VE-Cadherin (Cell Signaling Technology, Cat# 2500, 1:500) and ZO-1 (Invitrogen, Cat# 33-9100, 1:500) at 4 °C overnight, and the permeabilization step was omitted. The cells were washed with PBS twice for 10-min each and nuclear staining was performed with Hoechst 1:2000 in PBS incubation for 5 min at RT in the dark. After two 10-min PBS washes the cells were mounted and the slides were incubated for 2 h in the dark at RT and then stored at 4 °C in the dark till imaging (Confocal microscopy paragraph, below). Spots of VE-cadherin perpendicular orientation were manually quantified by two individual investigators in a blinded manner, and ZO-1 levels at the cell junctions were compared with the levels of the adjacent areas and three spots per cell were quantified. Quantification took place with ImageJ software (National Institutes of Health).

Confocal microscopy

Ear sponge sections

Fluorescent images were obtained with a multiphoton microscope (A1R; Nikon, NY, USA) in the confocal mode with Plan Apochromat Lamda 20X/0.75 numerical aperture air objective lenses. Each large image (showing the whole plug) was the outcome of stitching 12–16 images. Image acquisition and processing was controlled by Nikon NIS software.

Cell monolayers

Fluorescent images were obtained with a multiphoton microscope (A1R; Nikon, NY, USA) in the confocal mode with Plan Apochromat IR 60X/1.27 numerical aperture water immersion objective lenses. Image acquisition and processing was controlled by Nikon NIS software.

Statistical analysis

All experiments were repeated at least three times with similar results. Data analysis was performed using GraphPad Prism version 7.00 for Windows (GraphPad Software, San Diego, CA) and all results are expressed as mean \pm SEM. Statistical analysis was performed for two independent groups by Student's unpaired *t*-test, and for more than two independent groups by One-way ANOVA followed by Dunnett's multiple comparisons test. For the in vivo ear sponge assay statistical analysis was performed by a non-parametric Wilcoxon–Mann–Whitney test, as previously described [73, 74]. The asterisks in the figures denote statistical significance (NS: not significant, * $P < 0.05$; ** $P < 0.01$; *** $P < 0.001$).

Results

RhoA regulates Ang2-induced HDLEC migration

Given the varying functions of Ang2 in different conditions and cell types, we evaluated the impact of physiological Ang2 concentrations on the angiogenic and lymphangiogenic functions of HUVEC and HDLEC. To assess this, dose–response angiogenesis experiments for cell proliferation, migration and tube formation were conducted. In HUVEC, Ang2 had no effect on cell proliferation (Suppl. Fig. 1A), cell migration (Suppl. Fig. 1B), or sprout formation (Suppl. Fig. 1C–F) in the panel of concentrations tested. In the HDLEC, Ang2 caused a mild induction of cell proliferation (Suppl. Fig. 2A) but did not induce sprout formation in all concentrations tested (Suppl. Fig. 2B–E). The most profound effect of Ang2 treatment in vitro was observed

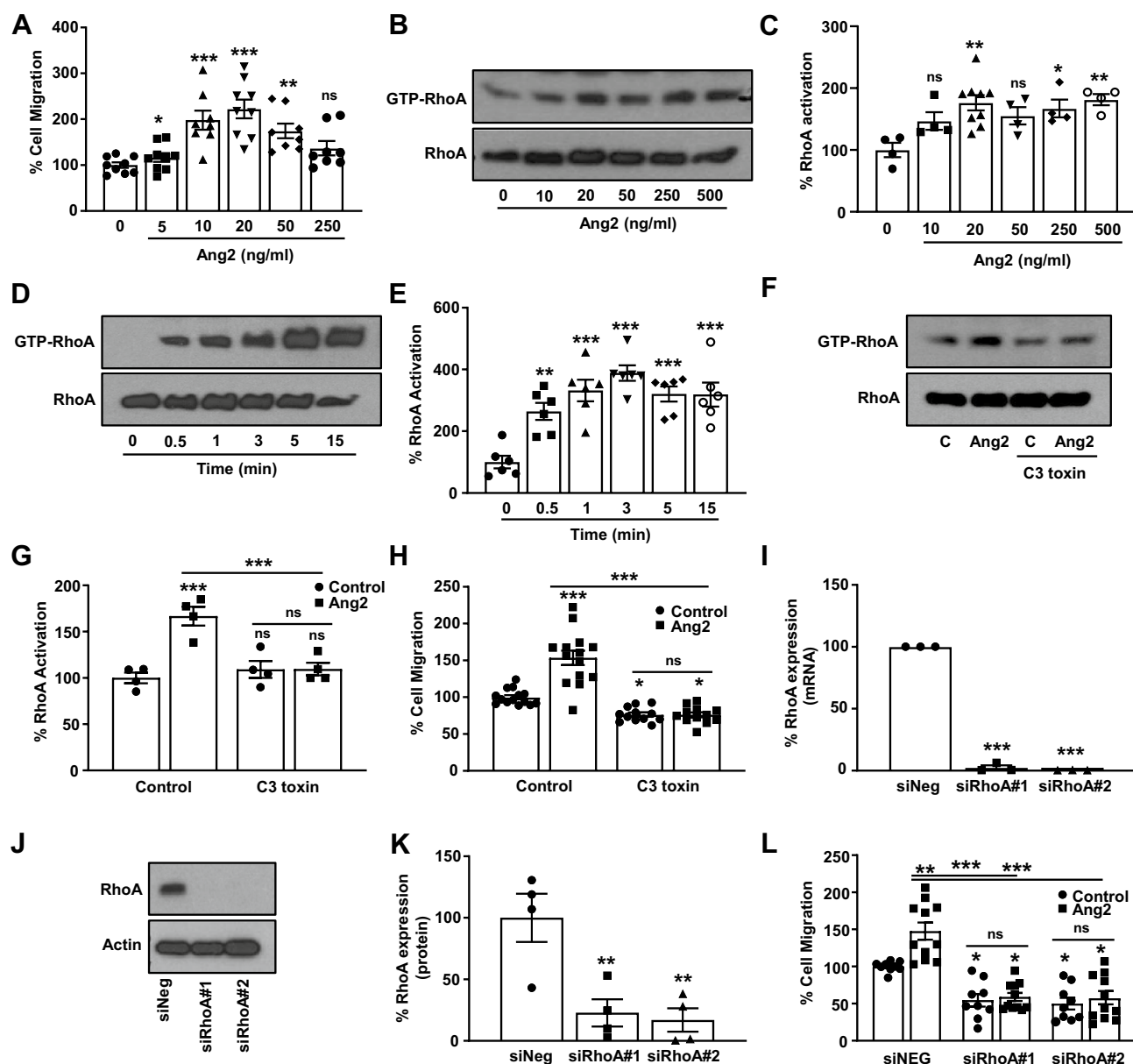


Fig. 1 Ang2-induced human dermal lymphatic endothelial cell (HDLEC) migration is regulated by RhoA. **A** Quantification of dose-response effect of Ang2 on HDLEC migration ($n=3$). **B**, **C** Representative images (**B**) and quantification (**C**) of RhoA activation ($n=4$). **D**, **E** Representative images (**D**) and quantification (**E**) of time-course experiments of Ang2- (20 ng/ml) driven RhoA activation ($n=6$). **F**, **G** Representative images (**F**) and quantification (**G**) of RhoA activation upon Ang2 (20 ng/ml) stimulation, in the presence or absence of C3 toxin (20 ng/ml) treatment ($n=4$). **H** Quan-

tification of Ang2-induced (20 ng/ml) cell migration in the presence or absence of C3 toxin (20 ng/ml) ($n=3$). **I** Quantification of RhoA mRNA levels 48 h after transfection of siRNA control (siNeg) or two sequences of siRNA for RhoA (siRhoA#1 and siRhoA#2) ($n=3$). **J**, **K** Representative images (**J**) and quantification (**K**) of RhoA protein expression 48 h after transfection of siNeg and siRhoA ($n=4$). **L** Quantification of Ang2-induced (20 ng/ml) cell migration of siNeg- and siRhoA-transfected cells ($n=3$). *ns* not significant; * $P < 0.05$; ** $P < 0.01$; *** $P < 0.001$

in the HDLEC migration, with significant differences at concentrations ranging from 10 to 50 ng/ml (Fig. 1A). This data somewhat agrees with Nguyen et al. [13], suggesting that, under the experimental conditions used, Ang2 induces LEC migration and proliferation, but has no effect on BECs,

emphasizing the diverse role of Ang2 in distinct vascular beds or endothelial cell types.

The small GTPase RhoA is mostly known for the regulatory role on actomyosin structure and dynamics and the regulation of stress fiber formation [41, 42], which are required for cell migration. To investigate whether Ang2

activates RhoA, we performed RhoA pull-down experiments upon treatment with different Ang2 concentrations for 3 min in HUVEC (Suppl. Fig. 3) and HDLEC (Fig. 1B, C). Even though Ang2 had no effect on HUVEC cell functions (Suppl. Fig. 1), it still induced a robust RhoA activation (Suppl. Fig. 3). In HDLEC, Ang2 treatment led to RhoA activation in as low as 20 ng/ml concentration (Fig. 1B, C). Time-course experiments of the selected Ang2 concentration (20 ng/ml) revealed that Ang2-induced RhoA activation occurs as early as 0.5 min and persists for longer than 15 min, with maximal activation occurring at 3 min, which was used for further experiments (Fig. 1D, E).

Active RhoA is a known inducer of cell migration [42, 44, 75, 76]. Since Ang2 induced RhoA activation and cell migration in the HDLEC, we further explored whether Ang2-induced HDLEC migration was RhoA-dependent. C3 toxin, a potent inhibitor of RhoA activation [77, 78], abrogated not only Ang2-induced RhoA activation (Fig. 1F, G) but also Ang2-induced cell migration (Fig. 1H), demonstrating that RhoA mediates Ang2-dependent HDLEC migration. To exclude potential confounding effects of RhoB or RhoC, which are also ADP-ribosylated by C3 toxin to a lesser extent [79], we knocked down RhoA expression in HDLEC by siRNA, as demonstrated by mRNA (Fig. 1I) and protein levels (Fig. 1J, K). RhoA knockdown also hindered Ang2-induced and basal cell migration (Fig. 1L), confirming the pharmacological inhibition findings and further verifying that RhoA is not only required for Ang2-induced cell migration but is an integral component of the migratory mechanism.

Ang2-induced HDLEC migration is independent of the Tie receptors

Ang2 directly interacts with the Tie2 receptor and indirectly with the Tie1 receptor [10, 80, 81]. To explore the involvement of the Tie receptors in Ang2-induced HDLEC migration we knocked down Tie1 and Tie2. Although Tie1 and Tie2 expression was significantly abrogated (Fig. 2A, B), RhoA activation upon Ang2 treatment was not significantly inhibited (Fig. 2C, D), with a similar effect observed in the cell migration experiments (Fig. 2E). However, the basal migratory levels in both conditions upon Tie1 knockdown presented an increasing trend. To account for the possibility of compensation among the Tie receptors, we performed double knockdown experiments for both Tie1 and Tie2 receptors. Double knockdown did not affect Ang2-induced RhoA activation, although the basal RhoA activation levels were increased upon double Tie1 and Tie2 deficiency (Fig. 2F, G). The cell migration experiments did not show a difference upon combined Tie1 and Tie2 deficiency either (Fig. 2H). It was previously reported that at high levels, Ang2 can phosphorylate the Tie2 receptor, activating the

PI3K/Akt pathway inducing cell migration [9]. However, a direct effect of Tie1 deletion on Ang2 expression has not been previously reported and considering the increased level of cell migration in the siTie1 group, we hypothesized that this could be due to a regulatory effect of the Tie1 receptor on Ang2 expression. To investigate this, Ang2 mRNA levels were measured upon the silencing of the Tie receptors. Ang2 mRNA levels were elevated upon Tie1 knockdown, but no change was seen with the Tie2 receptor knockdown (Fig. 2I). The slight increase in Ang2 expression upon Tie1 knockdown may not be the only accounting factor for the increase of the basal migratory potential of the LECs, but it seems to be a contributing one. The impact of Tie1 deficiency on Ang2-induced migration was not unexpected, as it is considered to have a redundant role on Ang2-induced functions [14]. However, Tie2 deficiency did not have the impact one would expect from a main receptor. To clarify the interaction between Ang2 and the Tie receptors, HDLEC were stimulated with Ang2 and immunoprecipitation experiments for each receptor were conducted to evaluate their activation upon Ang2 binding in HDLEC. As shown in Suppl. Fig. 4, Ang2 stimulation induced the phosphorylation of the Tie1 receptor but inhibited that of the Tie2 receptor. This signifies that the Tie receptors are dispensable for Ang2-induced LEC migration, suggesting the involvement of a different receptor.

Ang2-induced cell migration through RhoA involves beta-1 integrins

To identify the specific receptor interacting with Ang2, we treated HDLEC with Ang2 and performed immunoprecipitation for Ang2 and Tie2, followed by proteomic analysis of the brighter Coomassie-stained bands. These experiments highlighted integrin β 1, a transmembrane receptor whose interaction with Ang2 has been documented before [36, 82], which bound both to Ang2 and Tie2 (Suppl. Tables 1 and 2). After the identification of β 1 integrin by mass spec, the interaction between Ang2 and β 1 integrin was further illustrated by immunoprecipitation experiments (Suppl. Fig. 4C). To explore the role of β 1 integrin in Ang2-induced cell migration, we initially used a general integrin inhibitor, a peptide corresponding to the central-binding Arg-Gly-Asp (RGD) domain (RGD peptide) to inhibit integrin signaling [83]. Pretreatment with the RGD peptide reduced RhoA activation driven by Ang2 (Fig. 3A, B) and inhibited both basal and Ang2-induced cell migration (Fig. 3C). To confirm the involvement of β 1 integrin in Ang2-induced activities, β 1 integrin expression was knocked down (Fig. 3D, E) to evaluate Ang2-induced RhoA activation and HDLEC migration. Integrin β 1 deficiency attenuated Ang2-induced RhoA activation (Fig. 3F, G) and abrogated Ang2-induced HDLEC migration (Fig. 3H). The small but significant difference between the Ang2 treatment and control groups upon β 1

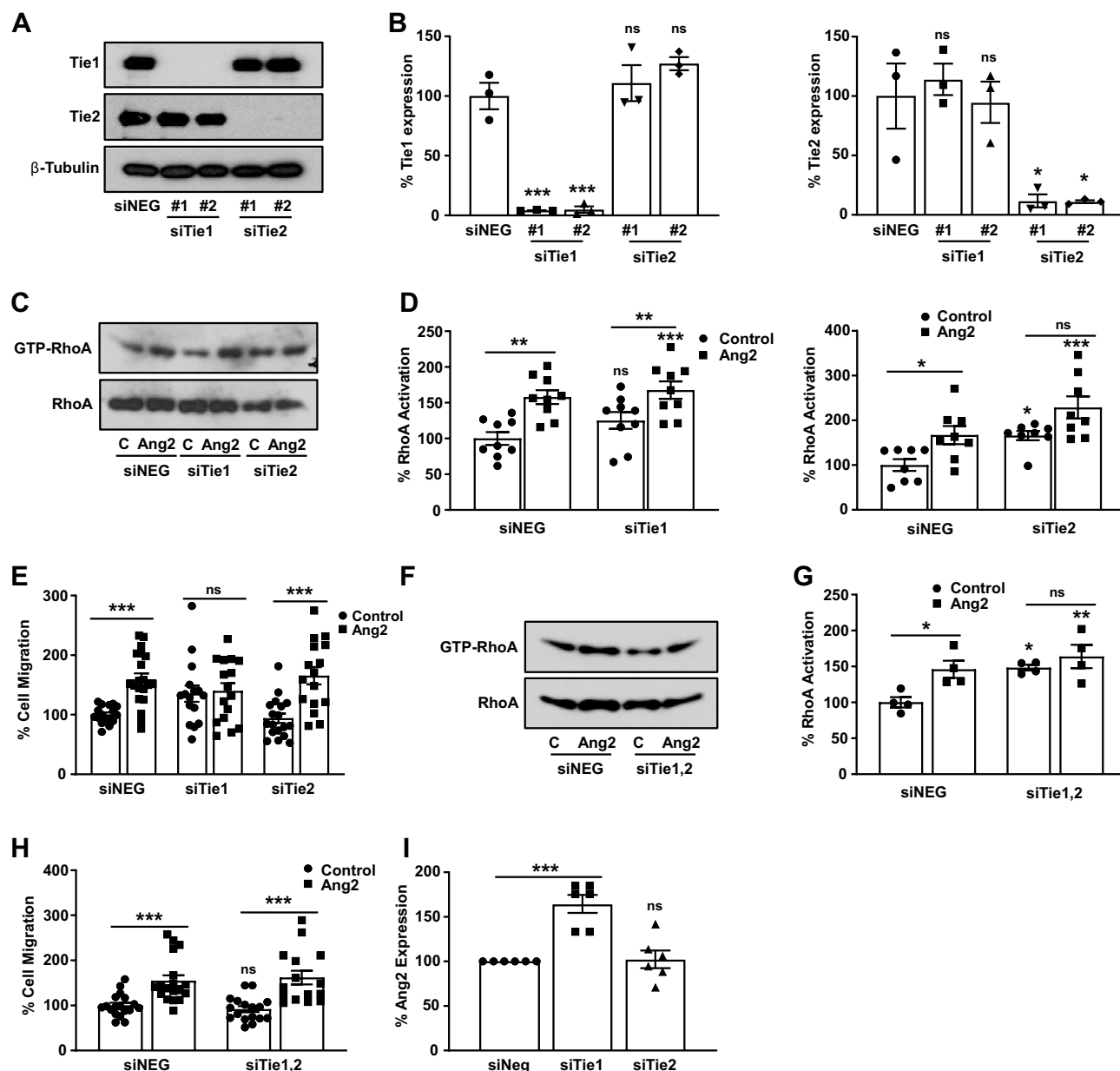


Fig. 2 Ang2-induced HDLEC migration is not dependent on the Tie receptors. **A**, **B** Representative images (**A**) and quantification (**B**) of Tie1 (left) and Tie2 (right) expression 48 h after transfection of siNeg, siTie1 or siTie2 ($n=3$). **C**, **D** Representative images (**C**) and quantification (**D**) of Ang2-induced RhoA activation of siNeg-, siTie1- or siTie2-transfected cells ($n=9$ for Tie1 and $n=8$ for Tie2 respectively). **E** Quantification of Ang2-induced cell migration of siNeg-, siTie1- or siTie2-transfected cells ($n=3$). **F**, **G** Representa-

tive images (**F**) and quantification (**G**) of RhoA activation upon Ang2 (20 ng/ml) stimulation in control (siNeg) or cells with combined Tie1 and Tie2 knockdown (siTie1,2) ($n=5$). **H** Quantification of Ang2-induced (20 ng/ml) cell migration of siNeg- and siTie1,2-transfected cells ($n=3$). **I** Quantification of Ang2 mRNA levels 48 h after transfection of siNeg, siTie1 or siTie2 ($n=2$). ns not significant; * $P < 0.05$; ** $P < 0.01$; *** $P < 0.001$

deficiency, could be partly due to the effect of the Tie receptors or other mediators, such as other integrins.

To clarify that and address the potential involvement of other integrins, we interrogated the role of downstream integrin signaling mediators. Focal adhesion kinase (FAK) and Src are important downstream integrin adaptors.

Integrin-mediated FAK activation induces a conformational change, allowing the autophosphorylation of Y397 residue of FAK and exposing the Src binding site. This induces the phosphorylation of additional sites on FAK, leading to its full activation and binding to the SH2 domain of Src, thus activating Src [84]. The activated FAK/Src complex

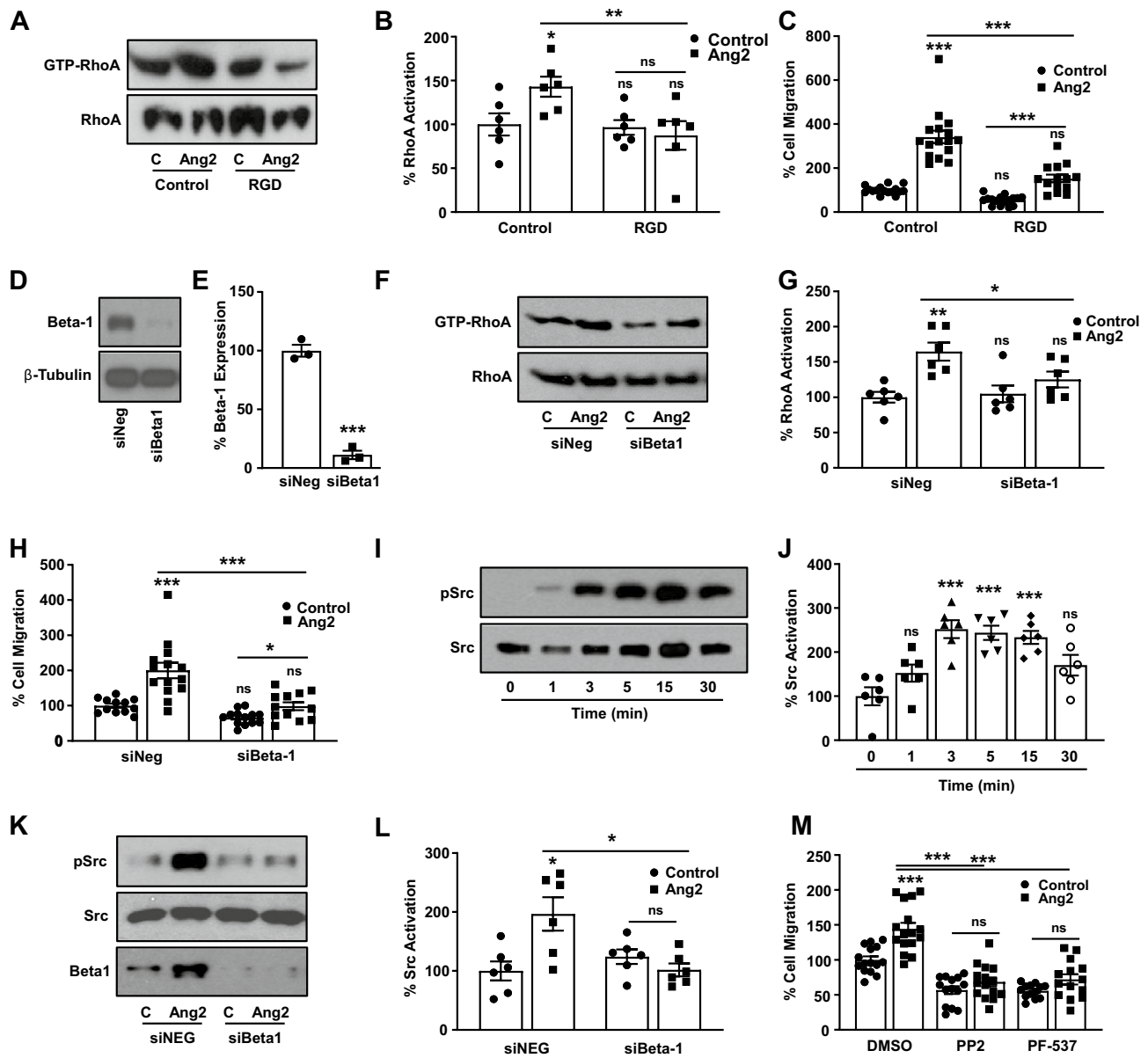


Fig. 3 Ang2-induced HDLEC migration and RhoA activation is regulated by $\beta 1$ integrin. **A, B** Representative images (**A**) and quantification (**B**) of RhoA activation upon Ang2 (20 ng/ml) stimulation, after preincubation of Control or RGD peptides ($n=6$). **C** Quantification of Ang2-induced (20 ng/ml) cell migration in the presence of Control or RGD peptide ($n=3$). **D, E** Representative images (**D**) and quantification (**E**) of beta1 integrin expression 48 h after transfection of siNeg and siBeta1 ($n=3$). **F, G** Representative images (**F**) and quantification (**G**) of RhoA activation upon Ang2 (20 ng/ml) stimulation in control (siNeg) or cells with beta1 integrin knockdown (siBeta1)

($n=6$). **H** Quantification of Ang2-induced (20 ng/ml) cell migration of control (siNeg) or Beta1-deficient (siBeta1) cells ($n=3$). **I, J** Representative images (**I**) and quantification (**J**) of time-course experiments of Ang2-induced (20 ng/ml) Src phosphorylation ($n=6$). **K, L** Representative images (**K**) and quantification (**L**) of Ang2-induced (20 ng/ml) Src phosphorylation in control (siNeg) or Beta1-deficient (siBeta1) cells ($n=6$). **M** Quantification of Ang2-induced (20 ng/ml) cell migration upon treatment with PP2 (10 μ M) and PF-573228 (PF-573) (5 μ M) ($n=3$). *ns* not significant * $P < 0.05$; ** $P < 0.01$; *** $P < 0.001$

regulates several functions, including cell migration [84]. Ang2 treatment of HDLEC induced a robust Src activation (Fig. 3I, J), which was abrogated upon $\beta 1$ integrin deficiency (Fig. 3K, L), demonstrating the dominant role $\beta 1$ integrin facilitates on Ang2-driven Src activation in the lymphatics. We then evaluated the impact of non-toxic doses of

PF-573228 (PF-573) and PP2 (Suppl. Fig. 5A–C), for FAK [85] and Src [86] inhibition respectively, on Ang2-induced HDLEC migration. As expected, the migratory potential driven by Ang2 was completely abrogated (Fig. 3M).

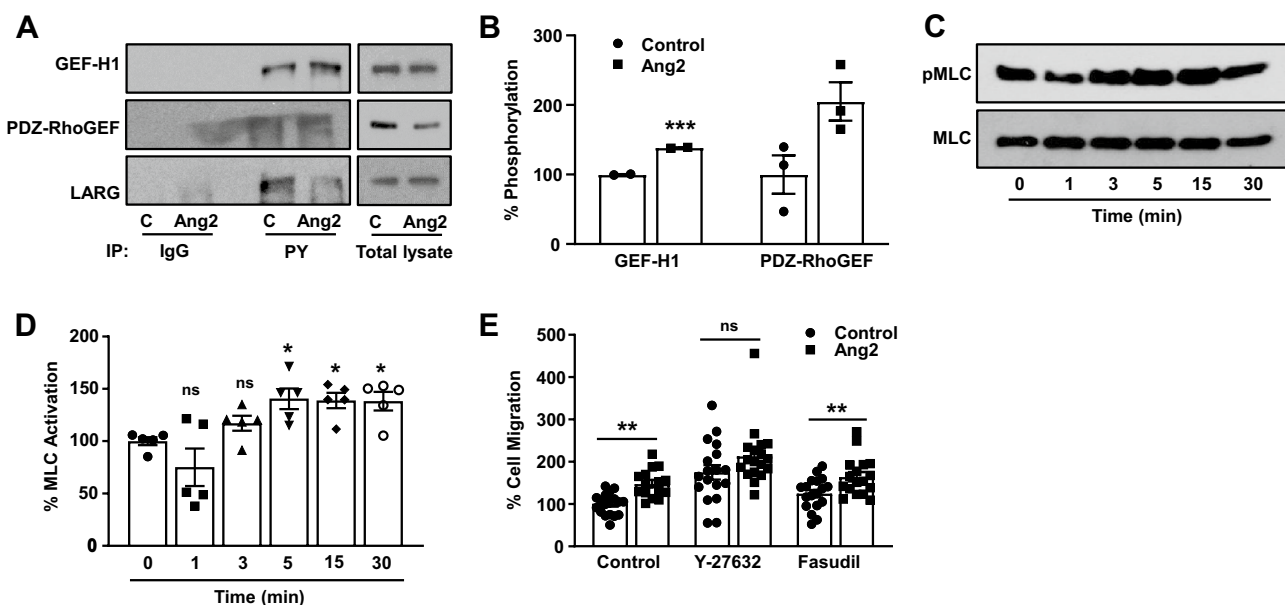


Fig. 4 ROCK inhibition does not block Ang2-induced HDLEC migration. **A**, **B** Representative images (**A**) and quantification (**B**) of GEF-H1 and PDZ-RhoGEF phosphorylation upon Ang2-induced (20 ng/ml) ($n=3$). **C**, **D** Representative images (**C**) and quantification (**D**) of time-course experiments of Ang2-induced (20 ng/ml)

MLC phosphorylation ($n=5$). **E** Quantification of Ang2-induced (20 ng/ml) cell migration upon treatment with Y-27632 (10 μ M) and Fasudil (10 μ M) ($n=3$). *ns* not significant; * $P < 0.05$; ** $P < 0.01$; *** $P < 0.001$

ROCK inhibition does not block Ang2-induced HDLEC migration

Rho GTPases cycle between an active, GTP-bound and an inactive, GDP-bound form. The activity of Rho GTPases is induced by Guanine nucleotide Exchange Factors (GEFs), which activate Rho proteins by catalyzing the exchange of GDP for GTP [87]. To further delineate the RhoA signaling cascade initiated upon Ang2- β 1 integrin interaction, we explored the RhoGEFs that induce RhoA activation, by checking the phosphorylation status of GEFs reported to be activated by integrin effectors, such as GEF-H1, PDZ-RhoGEF and LARG [88, 89]. Immunoprecipitation experiments using phospho-tyrosine antibody revealed that GEF-H1 is activated and PDZ-RhoGEF has a similar trend, whereas LARG does not seem to mediate Ang2-induced RhoA activation (Fig. 4A, B).

Key downstream RhoA effectors are Rho kinase (ROCK) and the myosin light chain (MLC), which are involved in the rearrangement of actin cytoskeleton [43, 90]. As expected, Ang2 induced MLC phosphorylation (Fig. 4C, D), signifying that it activates the ROCK/pMLC pathway. To confirm the involvement of this pathway on Ang2-driven HDLEC migration, we pharmacologically blocked the pathway with potent ROCK inhibitors Fasudil and Y-27632 in effective inhibitory concentrations [43]. Contrary to our expectations, neither Fasudil, nor Y-27632 inhibited Ang2-induced cell migration in different time points tested (Fig. 4E and Suppl.

Fig. 5D, E). Phalloidin staining in these time points did not reveal significant impact of the ROCK inhibitors on stress fiber formation in most conditions, which remained induced upon Ang2 stimulation (Suppl. Fig. 5F). These data suggest that although Ang2 activates the ROCK/pMLC pathway, this signaling cascade does not drive Ang2-mediated HDLEC migration.

FHOD1 mediates Ang2-induced HDLEC migration

Since ROCK inhibition does not mediate Ang2-induced HDLEC migration, we looked into alternative RhoA pathways, one of which involves formins, other known RhoA effectors [91], activated upon β 1 integrin-induced RhoA activation [92]. Formins polymerize actin filaments at the barbed end, controlling rearrangement of the actin cytoskeleton and regulating microtubule dynamics [93, 94]. To investigate whether formins mediate Ang2-RhoA-induced cell migration of HDLEC, we selected non-toxic doses of formin activator (IMM01) and inhibitor (SMIFH2) (Suppl. Fig. 6) and confirmed their effect on stress fiber formation. IMM01 treatment induced stress fiber formation while SMIFH2 treatment inhibited stress fiber formation in HDLEC, overcoming the effect of Ang2 (Fig. 5A). We then tested their effect on HDLEC cell migration, where IMM01 induced HDLEC migration irrespective of Ang2 stimulation and similarly SMIFH2 treatment completely abrogated HDLEC migration in both control and Ang2-treated groups (Fig. 5B),

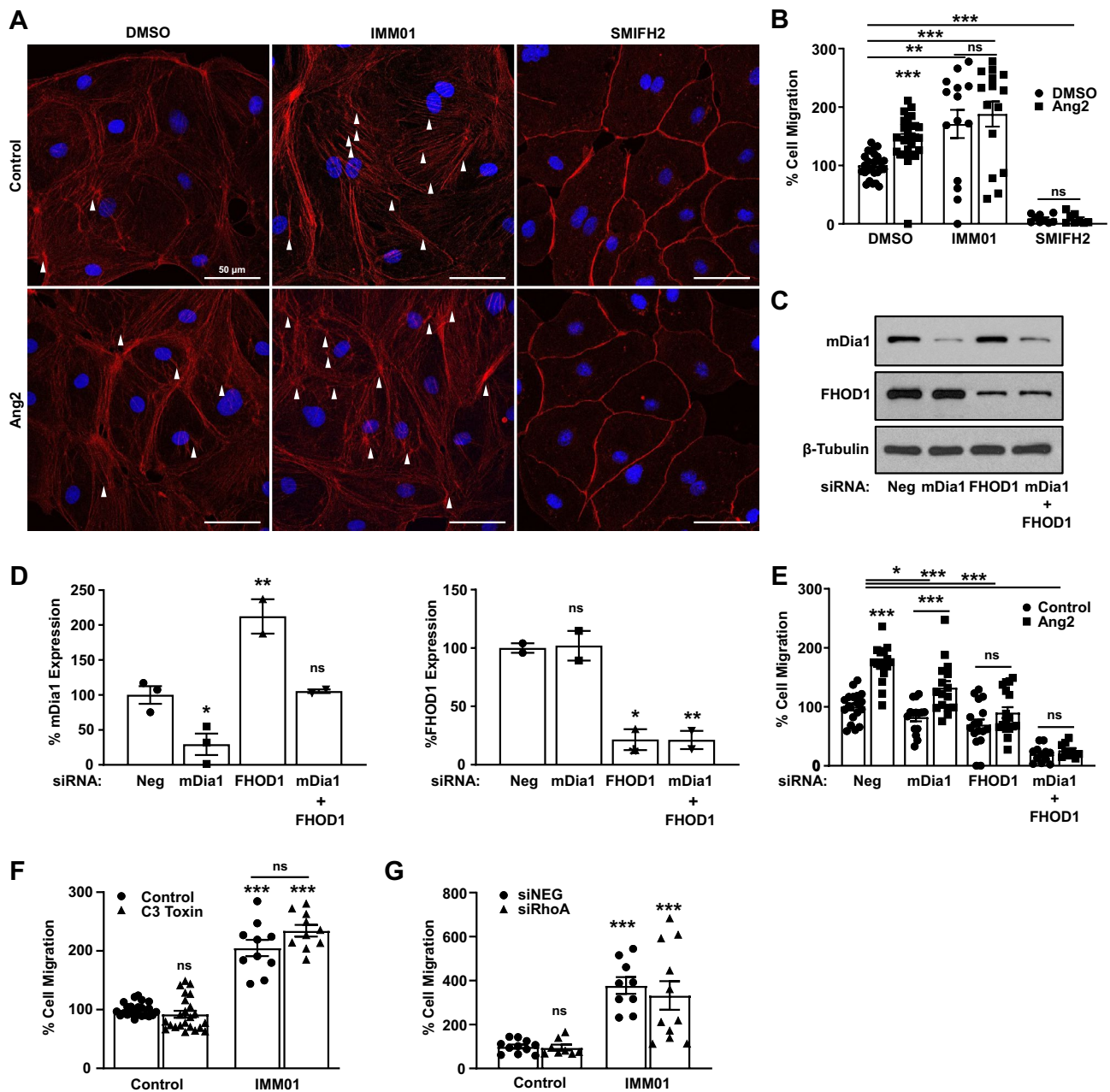


Fig. 5 Ang2-induced HDLEC migration is mediated by FHOD1. **A** Representative images of HDLEC with phalloidin staining (red) after treatment of Ang2 (20 ng/ml) and IMM01 (10 μ M) or SMIFH2 (5 μ M) ($n=3$) (blue: nuclei). White arrowheads denote representative stress fibers. **B** Quantification of Ang2-induced (20 ng/ml) cell migration with IMM01 (10 μ M) or SMIFH2 (5 μ M) treatment ($n=3$). **C, D** Representative images (**C**) and quantification (**D**) of mDia1 (left) and FHOD1 (right) expression 48 h after transfection with siNeg, simDia1, siFHOD1 and combination thereof ($n=3$ for mDia1; $n=2$ for

FHOD1). **E** Quantification of Ang2-induced (20 ng/ml) cell migration of control (siNeg), mDia1-deficient (simDia1), FHOD1-deficient (siFHOD1) or double mDia1, FHOD1-deficient cells ($n=3$). **F** Quantification of basal LEC migratory levels upon RhoA inhibition (C3 toxin; 20 ng/ml) in the presence (10 μ M) or absence of IMM01 ($n=3$). **G** Quantification of basal LEC migratory levels upon RhoA knockdown in the presence (10 μ M) or absence of IMM01 ($n=3$). *ns* not significant; * $P < 0.05$; ** $P < 0.01$; *** $P < 0.001$

demonstrating a critical role of formins on cell migration. Among the formins existing in mammals, mDia and FHOD1 are known to interact with RhoA [91, 92, 95]. Thus, we studied their effect on cell migration by knocking down their

expression (Fig. 5C). FHOD1 knockdown induced mDia1 expression in HDLEC, similar to what has been previously reported [92], signifying a compensatory mechanism. However, that was not the case for FHOD1 expression upon

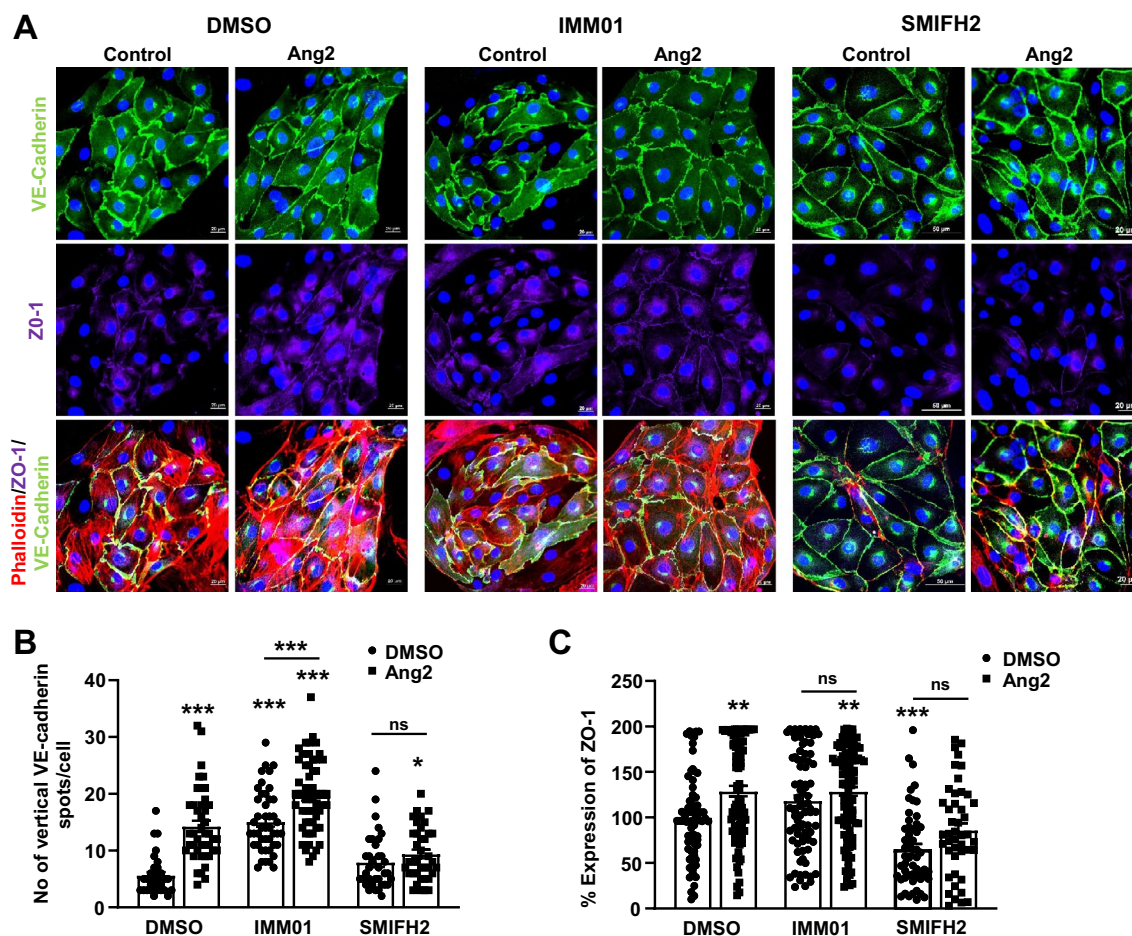


Fig. 6 Impact of formin activator and inhibitor on lymphatic endothelial cell junctions. **A** Representative images of HDLEC treated with/without Ang2 upon pretreatment with DMSO (control), IMM01 (10 μ M) or SMIFH2 (5 μ M) ($n=2$) (green: VE-cadherin; turquoise:

ZO-1; red: phalloidin; blue: nuclei). **B, C** Quantification of **(B)** number of vertical VE-cadherin orientation spots per cell and **(C)** ZO-1 staining in cell-to-cell junctions. *ns* not significant; ** $P < 0.01$; *** $P < 0.001$

mDia1 knockdown (Fig. 5C, D). Cell migration experiments verified the dominant role of FHOD1 on Ang2-induced cell migration (Fig. 5E). mDia1 knockdown had a limited, but significant, inhibitory effect on Ang2 stimulation, whereas upon FHOD1 knockdown, the cell migration was reduced to the basal levels. Double mDia1 and FHOD1 knockdown blocked even the basal levels of HDLEC migration. Altogether, these results demonstrate that Ang2 regulates the HDLEC migratory potential via $\beta 1$ integrin-mediated RhoA activation and formin-, mostly FHOD1-induced stress fiber formation, independently of the classical ROCK/pMLC pathway. As a rescue experiment to further evaluate that the formin pathway is in the same axis with the RhoA pathway, we performed cell migration experiments testing the impact of formin activation (IMM01 treatment) upon pharmacological inhibition of RhoA signaling by C3 toxin (Fig. 5F) or RhoA knockdown (Fig. 5G). Formin activation rescued the RhoA signaling inhibition in both approaches, confirming them as the downstream mediators of LEC migration.

The striking impact of the formin activation and inhibition on HDLEC stress fiber formation prompted us to evaluate their effect on LEC junction morphology (Fig. 6A). Ang2 induced a mild disorganization of LEC junctions, in terms of increased junction zippering via VE-cadherin perpendicular orientation and decreased ZO-1 levels, which was significantly induced by formin activation (Fig. 6A, B). Formin inhibition blocked this disorganization and led to straighter junctions and limited ZO-1 expression (Fig. 6A, B), demonstrating the potential impact of Ang2-induced formin regulation on junctional assembly and function.

Lymphatic endothelial RhoA deficiency abrogates Ang2-induced lymphangiogenesis

Since Ang2 induces HDLEC migration, we aimed to evaluate its role on lymphangiogenesis. Using the ear sponge assay as an *in vivo* lymphangiogenesis model (Suppl. Fig. 7A) [72, 73], we evaluated whether murine Ang2 had

lymphangiogenic potential in the implanted ear sponges after 14 (Fig. 7A, B) and 21 (Suppl. Fig. 7B, C) days of implantation. Lymphatic vessels were identified by Lyve-1 staining and were positive for Tie2 (Suppl. Fig. 7D). In both incubation periods, Ang2 presented a lymphangiogenic effect, assessed by the quantification of lymphatic vessel area and density. In 21 days, Ang2 induced a significant increase of lymphatic vessel density and a tendency of increased lymphatic vessel area (Suppl. Fig. 7C), while in 14 days, the outcome was more pronounced and both parameters were significant (Fig. 7B). Therefore, we selected the 14-day incubation period as a more favorable time point for the in vivo experiments. To define the impact of lymphatic endothelial RhoA deficiency on Ang2-induced lymphangiogenesis, we engineered mice with conditional RhoA deficiency under the control of *Prox1-CreER^{T2}* promoter (*RhoA^{ff}; Tom-GFP^{ff}; Prox1-CreER^{T2}*). Excision efficiency was monitored by RhoA expression levels upon dermal LEC isolation (Suppl. Fig. 7E). For local, ear-specific lymphatic excision efficiency for our model, we used the tdTomato-GFP reporter [96], where LECs can be visualized as GFP-expressing structures upon Cre-mediated gene recombination (Fig. 7C, D). Intravital imaging of the ear dorsal skin area after tamoxifen treatment revealed significant excision efficiency, assessed by GFP expression (Fig. 7D), allowing us to proceed with further experiments. Lymphatic endothelial RhoA deficiency inhibited Ang2-induced in vivo lymphangiogenesis (Fig. 7E), assessed by lymphatic vessel area and lymphatic vessel density (Fig. 7F), demonstrating that RhoA is a significant mediator of Ang2-induced lymphangiogenesis.

The high potency of the formin inhibitor SMIFH2 on HDLEC migration prompted us to test its effect on Ang2-driven lymphangiogenesis in the ear sponge assay and, thus, performed a dose–response experiment with smaller doses than normally published [97, 98]. Both concentrations did not show toxicity, demonstrated by the number of the recruited cells (assessed by the stained nuclei) in the ear sponges (Fig. 8A). The 10 μ M concentration was able to block lymphatic vessel density and at higher concentration both lymphatic growth parameters (lymphatic vessel area and density) were inhibited (Fig. 8B).

Discussion

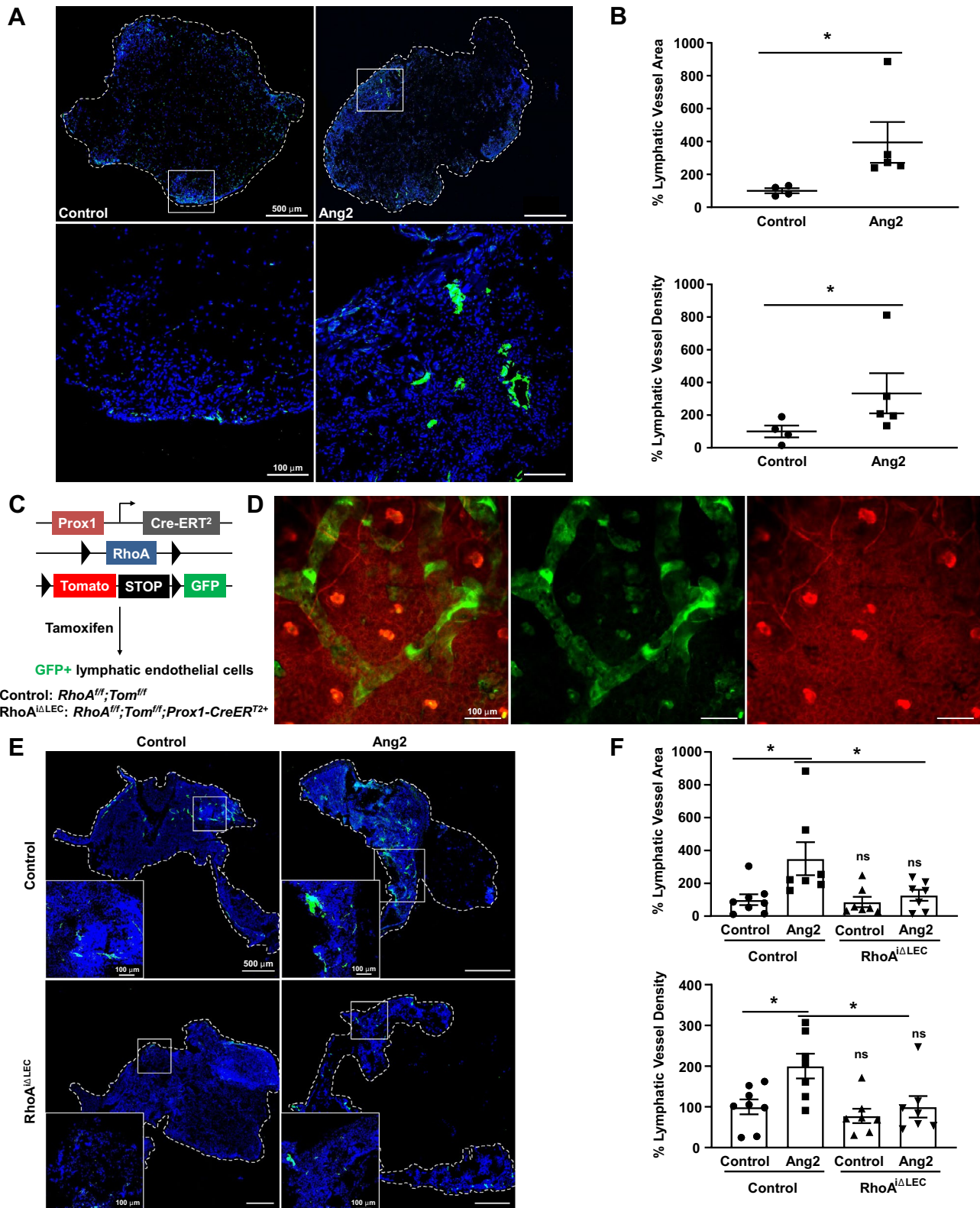
The Ang/Tie signaling pathway is a significant regulator of angiogenesis. Ang2 levels are upregulated and have prognostic value in various inflammatory conditions, including lung injury, sepsis [99] and tumors. In tumors, increased Ang2 levels have been positively correlated with tumor angiogenesis and metastasis, since both were reduced upon Ang2 inhibition [100–102]. Here, we show that Ang2 activates RhoA and that Ang2-induced RhoA activation mediates

LEC migration and lymphangiogenesis via formins FHOD1 and mDia1 (Fig. 9). We elucidated the pathway activated by Ang2 and highlighted the signaling elements that can be targeted for lymphangiogenesis inhibition.

Despite the central role of the Ang/Tie signaling pathway, previous contradicting studies have pinpointed this pathway's complexity, and some have revealed the context-dependent Ang2 effects. Some studies observed that Ang2 had no angiogenic effect or acted as an antagonist to Ang1 [2, 8], and other studies reported that Ang2 induces angiogenesis and lymphangiogenesis, showing its role as an agonist [7–9, 11–13]. However, the angiogenic effects of Ang2 have only been observed at high concentrations [103, 104]. In diseased conditions, such as cancer and systemic sclerosis, serum Ang2 levels are significantly elevated than in steady state conditions [103, 105, 106]. We now report cellular activity and signaling pathways of lower, near clinically observed, Ang2 concentrations, providing higher clinical relevance.

RhoA is among the most conserved Rho GTPases in mammals [107]. It regulates cytoskeletal changes promoting stress fiber formation, focal adhesion assembly [108], coordinating cellular processes, such as cell migration [42, 44–46, 75, 76] and cell retraction [42], which in endothelial cells can be translated as induction of permeability [43, 109]. The other ligand of the Ang/Tie family, Ang1, has been shown to either activate or inhibit RhoA; Ang1-driven RhoA activation induced cell motility [110], while its inhibition coupled with Rac1 activation inhibited vascular leakage in vivo [111]. Contrary to the Ang1-RhoA association, a potential relationship between Ang2 and RhoA has not been previously reported. The ability of Ang2 to induce RhoA activation in HUVEC was unexpected, since neither we, nor others, have observed biological activity in BECs in vitro in such low Ang2 concentrations and will be further explored. We attribute the difference in the biological outcome of Ang2-induced RhoA activation among blood and LECs to the presence of diverse regulatory mechanism(s), which would allow the differential outcome of RhoA activation in each cell type. A characteristic example would be the vascular endothelial protein tyrosine phosphatase (VEPTP), whose presence has been elegantly shown to block Ang2-induced Tie2 activation in HUVEC [112]. In terms of receptor phosphorylation, although the inhibition of the Tie2 phosphorylation by Ang2 is not unexpected [2], the increased Tie1 phosphorylation was, and the significance of which would be worth studying in the future.

Integrins are heterodimeric transmembrane proteins functioning as cellular receptors for extracellular matrix and are pivotal for cell migration through their interaction with signaling molecules or adaptors, such as focal adhesions [113]. Apart from extracellular matrix proteins, integrins act as receptors or co-receptors for growth factors [63,



114] and cytokines [115]. Ang2 has been shown to interact, directly or indirectly, with integrins in different cell types [36, 116–119]. Integrins can recognize and bind to specific

motifs through the central-binding domain Arg-Gly-Asp (RGD). RGD is a sequence of the cell attachment site for several adhesive extracellular matrix, blood, and cell surface

Fig. 7 Lymphatic endothelial RhoA deficiency abrogates Ang2-induced lymphangiogenesis. **A, B** Representative images (**B**) and quantification of lymphangiogenesis (assessed as lymphatic vessel area and density) in vehicle- and Ang2-treated sponges 14 days after sponge implantation ($n=2$). Scale bars, 500 μm at the top and 100 μm at the bottom row. **C** Schematic representation of lymphatic endothelial-specific conditional RhoA-deficiency with the Tomato-GFP reporter. **D** Representative confocal images of mouse ear of Tamoxifen-treated $\text{RhoA}^{\text{fl/fl}}$; Tomato-GFP $^{\text{fl/fl}}$; Prox1-CreERT 2 + mouse showing excision efficiency driven by the Prox1-CreERT 2 promoter (GFP+lymphatic capillaries are shown among all the other mouse cells that are RFP+). Scale bars, 100 μm . **E, F** Representative images (**E**) and quantification of lymphatic vessel area and density (**F**) in vehicle- and Ang2-treated sponges in $\text{RhoA}^{\text{iALEC}}$ and littermate control mice 14 days after implantation. *ns* not significant; * $P < 0.05$

proteins. Peptides, such as RGD, promote cell adhesion when insolubilized onto a surface, and inhibit it when presented to cells in soluble form [83, 120]. In our experiments, pretreatment with RGD inhibited both basal and Ang2-induced lymphatic endothelial migration, demonstrating the significance of integrins in Ang2-driven functions. The difference between control and Ang2 groups under RGD treatment could be attributed to either insufficient inhibition by the RGD peptide or other unexplored pathways.

$\beta 1$ integrin is an established Ang2 receptor. In the absence of Tie2, Ang2 also interacts with $\beta 1$ integrin, exerting angiogenic activity through FAK and Rac1 activation [36]. Our protein sequencing analysis revealed that $\beta 1$ integrin binds with both Tie2 and Ang2 in the same complex.

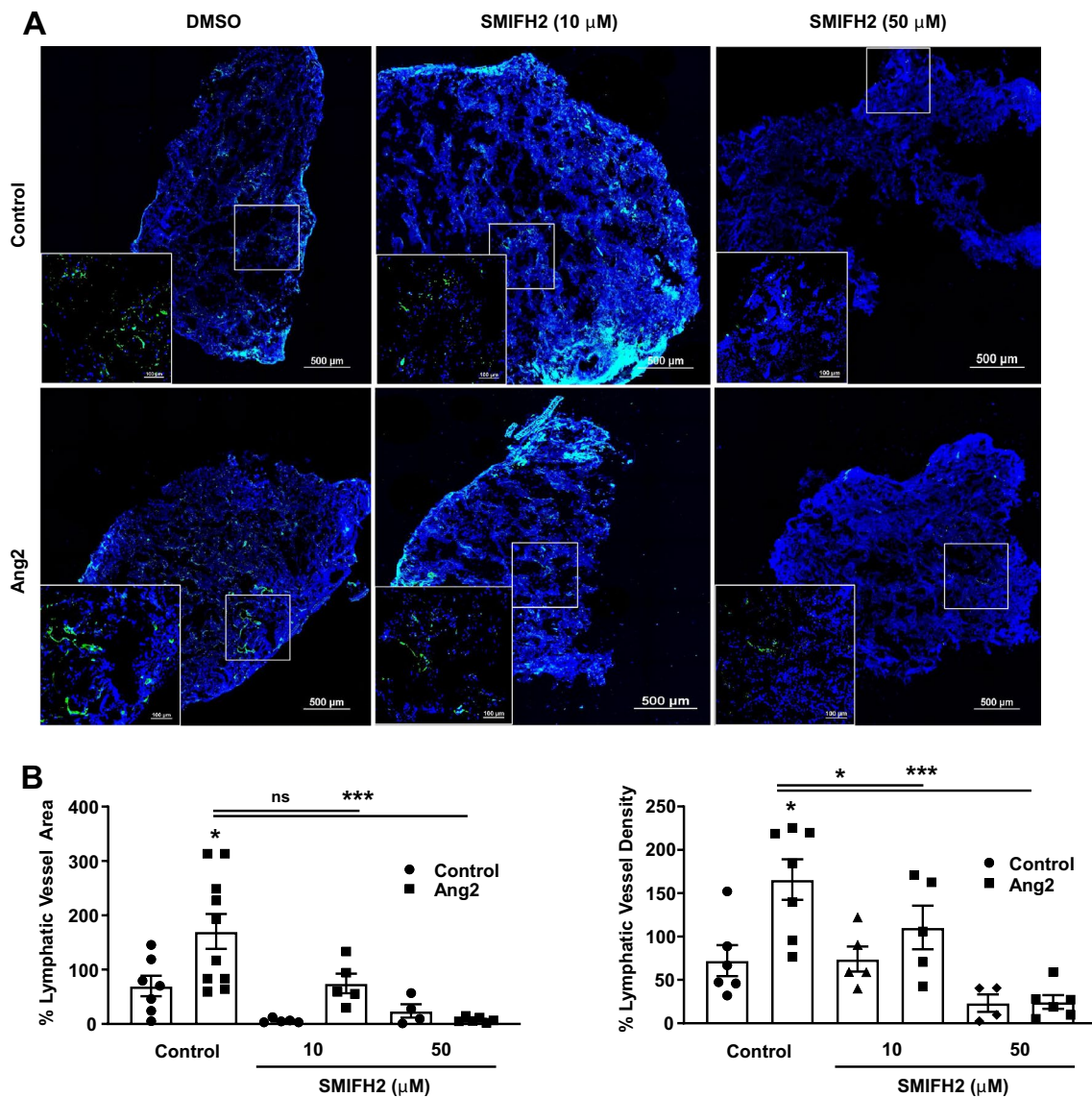


Fig. 8 The formin inhibitor SMIFH2 blocks basal and Ang2-induced lymphangiogenesis. **A** Representative images and **B** quantification of lymphangiogenesis (assessed as lymphatic vessel area and density) in

DMSO and SMIFH2-treated sponges 14 days after sponge implantation ($n=1$). Scale bars, 500 μm at the main and 100 μm at the magnified images. *ns* not significant; * $P < 0.05$; *** $P < 0.001$

Moreover, the Tie receptor single and double knockdown experiments revealed that: (i) Ang2 activates integrin-mediated cell migration irrespectively of the presence of Tie2 and (ii) the possibility that Tie1 receptor is participating in the cell migration machinery, since its deletion induced basal cell migration. Although the increasing trend upon Tie1 knockdown was obvious, this increase was not statistically significant. The increase of Ang2 expression obtained upon Tie1 knockdown justifies this trend, though this poses the question whether Tie1 deficiency has an effect only on Ang2 expression or it affects the expression of other cytokines/growth factors, thus signaling pathways. It has also been shown that upon Tie2 silencing, Ang2 activates β 1 integrin leading to endothelial destabilization, which was rescued by ROCK inhibition, implying the functional involvement of RhoA and downstream ROCK/pMLC signaling in this system [82]. However, in our case, although the ROCK/pMLC pathway was activated, it was not functionally significant for cell migration, as ROCK inhibition did not block it, demonstrating that different Ang2-integrin-driven RhoA downstream mediators regulate this function.

Rho GTPases are activated by GEFs, which activate Rho proteins by catalyzing the exchange of GDP for GTP [87, 121]. Trying to delineate the pathway that leads to RhoA activation downstream of β 1 integrin activation, we explored the involvement of GEFs. GEF phosphorylation is one of the dominant ways for their activation [89], and as such, we found that Ang2 phosphorylates GEF-H1 and seems to partially activate PDZ-RhoGEF, although this trend did not reach statistical significance. GEF-H1 is activated downstream of the FAK-Raf signaling pathway [88], and PDZ-RhoGEF is known to interact and thus be phosphorylated by FAK [122]. The activation of the Src/FAK complex downstream of Ang2-bound β 1 integrin, as well as the abrogation of the Src phosphorylation, RhoA activation and cell migration upon β 1 integrin silencing support the hypothesis of the Ang2-driven, β 1 integrin-mediated phosphorylation of these GEFs and thus RhoA activation. Downstream of RhoA activation, the differential effect of ROCK inhibitors is of interest, with a higher basal migratory potential upon Y-27632 treatment. Differences between the two tested ROCK inhibitors were identified in different treatment periods and we speculate that this could be due to the diverse nature of each inhibitor and potential alternative targets one of both may have, although this needs to be experimentally confirmed.

During cell migration, cells acquire a polarized morphology clearly indicating the front and the back end of the cell [123]. One of the events during this polarization is the formation of filamentous, F-actin. Formins are potent regulators of actin dynamics, containing a series of domains and functional motifs. Some formins are regulated by auto-inhibition through interaction between the diaphanous inhibitory domain (DID) and diaphanous auto-regulatory

domain (DAD), and activated by Rho GTPase binding to the GTPase-binding domains (GBD) [124, 125]. The Ang/Tie family is known to activate formins, as Ang1 was shown to prevent VEGF-induced endothelial permeability by inhibiting VEGF-induced activation of Src through Ang1-induced RhoA activation, which then activated mDia, resulting to its association with Src [91]. Since mDia and FHOD1 are the two formins known to interact with RhoA [92, 95, 126], we focused our study on these two formins, revealing the dominant role of FHOD1 on Ang2-driven LEC migration. Although this may not be the only pathway for Ang2-driven LEC migration, it seems to impact this process.

Ang2 induces its effect on endothelial cells via both autocrine and paracrine mechanisms [7, 9, 13, 34–36, 127]. Our data showed that endothelial RhoA inhibition is a limiting factor for Ang2-induced lymphangiogenesis *in vivo*. Both *in vitro* and *in vivo* assays were based on paracrine (exogenous addition of Ang2), although, since endothelial cells are Ang2 producers, autocrine effect in both cases could not be excluded. Lymphangiogenesis observed in the ear sponge assay can be attributed to both the autocrine and paracrine effects of Ang2. Due to the paracrine/chemotactic effect of exogenous Ang2, the LECs migrated towards Ang2 in the sponge generating the initial lymphangiogenic outcome. Due to the limited half-life of an exogenously added protein, the continued induction of lymphangiogenesis can be attributed to the autocrine effect of Ang2 in the LECs. It was recently shown in retinal angiogenesis studies that Cre-mediated toxicity is likely to confound the interpretation of angiogenesis outcome. Reduced retinal vascular parameters were observed in tamoxifen-injected pups expressing CreERT2 with or without the presence of floxed genes [128, 129]. Whether this is the case in lymphangiogenesis has not yet been explored and is an area worth investigating. In our study, both the wild type (control) and RhoA floxed (lymphatic endothelial RhoA-deficient) mouse pups were treated with tamoxifen. While this may eliminate potential questioning regarding toxicity from tamoxifen treatment, it does not answer the possibility of CreERT2 toxicity in lymphangiogenesis.

Overall, our findings highlighted the role of the small GTPase RhoA in Ang2-driven LEC functions *in vitro* and *in vivo*, delineated the signaling pathway and provided new targets for inhibition of aberrant lymphangiogenesis, which is characteristic of several inflammatory conditions. This newly discovered relationship between RhoA and Ang2 opens up translational implications for targeting Ang2-driven vascular activity. RhoA is a common downstream regulator of the VEGF-A/VEGFR2 [44–47], VEGF-C/VEGFR3 [51, 52, 130] and now the Ang/Tie signaling. Inhibition of RhoA blocks the activity of all these pathways, which could account for the observed resistance with VEGF/

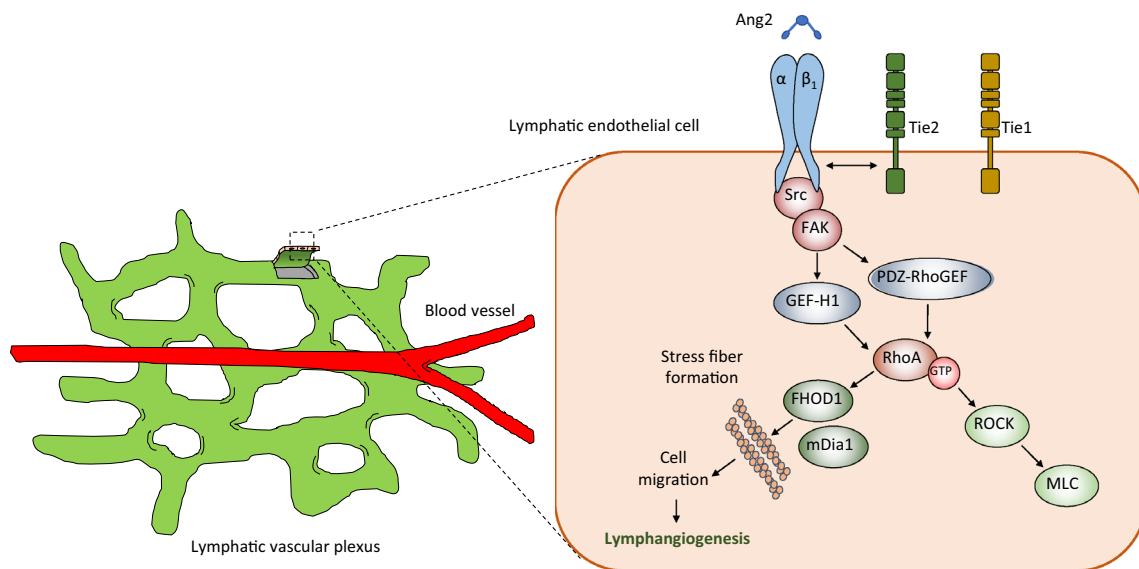


Fig. 9 Schematic representation of the signaling pathway regulating Ang2-induced lymphatic endothelial cell migration and lymphangiogenesis. Ang2 binding to beta1 integrin activates Src and FAK, which leads to RhoA activation via GEF-H1 and PDZ-RhoGEF phosphorylation. RhoA activation phosphorylates both ROCK and formins, the

downstream effectors. ROCK-MLC signaling does not regulate cell migration, which is instead regulated by FHOD1 and mDia1. RhoA is a mediator of Ang2-induced lymphatic endothelial cell migration and lymphangiogenesis

VEGFR targeting therapies, suggesting the inhibition of a common downstream target as a more effective option.

Appendix

Key Resources Table

Reagents or resources	Source	Identifier
Cells and media		
HDLEC	PromoCell	Cat# C-12216
Endothelial cell growth supplement	R&D systems	Cat# CCM027
Endothelial cell base growth media	R&D systems	Cat# CCM028
M199 medium	Corning	Cat# MT10060CV
Fetal Bovine Serum	GIBCO™	Cat# 10438026
DMEM	Life Technologies Corporation	Cat# 11995073
Antibodies		
RhoA (67B9)	Cell Signaling Technology	Cat# 2117; RRID: AB_1069392
Tie1 (D2K2T)	Cell Signaling Technology	Cat# 23111; RRID: AB_2798856
Tie2	R&D Systems	Cat# AF313; RRID: AB_355295
Integrin beta-1 (D6S1W)	Cell Signaling Technology	Cat# 34971; RRID: AB_2799067
mDia1 (Diap1)	Cell Signaling Technology	Cat# 5486; RRID: AB_10828440
FHOD1	ECM Biosciences	Cat# FM3521; RRID: AB_2104508
Angiopoietin-2	Cell Signaling Technology	Cat# 2948; RRID: AB_2289507

Reagents or resources	Source	Identifier
Angiopoietin-2	Santa Cruz Biotechnology	Cat# sc-74403, RRID: AB_1118956
Tubulin	Cell Signaling Technology	Cat# 2146; RRID: AB_2210545
Actin	Cell Signaling Technology	Cat# 3700; RRID: AB_2242334
GEF-H1	Cell Signaling Technology	Cat# 4076; RRID: AB_2060032
PDZ-Rho GEF	Abcam	Cat# ab110059; RRID: AB_10863676
LARG	Abcam	Cat# ab136072; RRID: AB_2828035
FAK	Cell Signaling Technology	Cat# 3285; RRID: AB_2269034
Phospho-FAK (Tyr397) (D20B1)	Cell Signaling Technology	Cat# 8556; RRID: AB_10891442
Src	Cell Signaling Technology	Cat# 2108; RRID: AB_331137
Phospho-Src	Cell Signaling Technology	Cat# 2101; RRID: AB_331697
Myosin light chain 2	Cell Signaling Technology	Cat# 3672; RRID: AB_10692513
Phospho-myosin light chain 2	Cell Signaling Technology	Cat# 3674; RRID: AB_2147464
Akt	Cell Signaling Technology	Cat# 9272; RRID: AB_329827
Phospho-Akt (Ser473)	Cell Signaling Technology	Cat# 4060; RRID: AB_2315049
PY—4G10	Millipore	Cat# 05-1050X; RRID: AB_916370
Anti-rabbit	Southern Biotech	Cat# 4010-05; RRID: AB_2632593
Anti-goat	Southern Biotech	Cat# 6420-05; RRID: AB_2796335
Anti-mouse	Southern Biotech	Cat# 1010-05; RRID: AB_2728714
LYVE1	R&D systems	Cat# AF2125; RRID: AB_2297188
IgG mouse isotype control	Santa Cruz Biotechnology	Cat# sc-2025; RRID: AB_737182
LYVE-1	ReliaTech	Cat# 103-PA50; RRID: AB_2783787
VE-cadherin	Cell Signaling Technology	Cat# 2500; RRID: AB_10839118
ZO-1	Invitrogen	Cat# 33-9100; RRID: AB_87181
siRNAs		
RhoA 1, s758	Ambion	Cat# 4390826
RhoA 2, s759	Ambion	Cat# 4390826
Tie1 a, s14142	Ambion	Cat# 4392420
Tie1 b, s14141	Ambion	Cat# 4392420
Tie 2 a, s13984	Ambion	Cat# 4457298
Tie 2 b, s13984	Ambion	Cat# 4390824
Integrin beta 3, s7575	Ambion	Cat# 4390824
Integrin beta 1, s112581	Ambion	Cat# AM51331
mDia1	Dharmacon	Cat# M-010347-02-0005
FHOD1	Dharmacon	Cat# M-013709-01-0005
Silencer® Select Negative Control siRNA	Thermo Fisher Scientific	Cat# 4390844
Other reagents & materials		
DharmaFECT 1	Dharmacon	Cat# T-2001
Tamoxifen	Alfa-Aesar	Cat# 10540-29-1
JumpStart REDTaq Ready-Mix Reaction Mix	Millipore Sigma	Cat# P0982-100-RXN
Antibiotic–antimycotic solution	GIBCO™	Cat# 15240-062
Glutathione Sepharose 4B beads	GE-Healthcare	Cat# 45-000-139
Protease and phosphatase inhibitor cocktail	Thermo Scientific	Cat# 1861281
Immobilon Western Chemiluminescent HRP substrate	Millipore	Cat# WBKLS0500
Immobilon P	Millipore	Cat# IPVH304F0
Polycarbonate membranes	NeuroProbe	Cat# PFB8
Trypsin–EDTA	Life Technologies	Cat# 25300-054

Reagents or resources	Source	Identifier
RGF-basement membrane extract	Trevigen	Cat# 3433
Qiagen's RNeasy mini kit	Qiagen	Cat# 74101
Verso cDNA synthesis kit	Thermo Scientific	Cat# AB-14531/A
SYBR Green PCR MasterMix	Thermo Fisher Scientific	Cat# 4309155
Dyna beads A	Invitrogen	Cat# 10004D
Dyna beads G	Invitrogen	Cat# 10002D
Human Ang2	Peptotech	Cat# 130-07
Mouse Ang2	Fisher Scientific	Cat# 7186-AN
C3 toxin	Fisher Scientific	Cat# NC9317720
RGD	Fisher Scientific	Cat# NC0210557
PP2	Fisher Scientific	Cat# 52-957-31MG
PF-573228	Fisher Scientific	Cat# 50-101-3643
SU-6656	Fisher Scientific	Cat# 57-263-51MG
Y-27632	Fisher Scientific	Cat# 12-541-0
Fasudil	LC Laboratories	Cat# F4660
IMM01	Sigma Aldrich	Cat# SML1064
SMIFH2	Sigma Aldrich	Cat# S4826
Dispase	Fisher Scientific	Cat# 17105-041
Collagenase Type II	Fisher Scientific	Cat# 17101-015
qPCR oligonucleotides (<i>Primers</i>)		
Human RhoA Forward: 5'-AGC CAAGATGAAGCAGGA GC-3'	Integrated DNA Technologies	
Human RhoA Reverse: 5'-TTCCCACGTCTAGCTTGCAG-3'	Integrated DNA Technologies	Integrated DNA Technologies
Human Ang2 Forward: 5'-AAGAGAAAGATCAGCTACAGG-3'	Integrated DNA Technologies	Integrated DNA Technologies
Human Ang2 Reverse: 5'- CCTAGAGTTTGATGTGGAC-3'	Integrated DNA Technologies	Integrated DNA Technologies
Human Actin Forward: 5'-CTCTTCCAGCCTTCCTTCTTG-3'	Integrated DNA Technologies	Integrated DNA Technologies
Human Actin Reverse: 5'- CAGCACTGTGTTGGCGTACAG-3'	Integrated DNA Technologies	Integrated DNA Technologies
Genotyping oligonucleotides (<i>Primers</i>)		
RhoA ^{fl/fl} Forward: 5'-TCTCTGCACTGAGGGAGTTAGG-3'	Integrated DNA Technologies	Integrated DNA Technologies
RhoA ^{fl/fl} Reverse: 5'-GTACATACAGGGAATGGAAACAAGG-3'	Integrated DNA Technologies	Integrated DNA Technologies
Tom-GFP Wt Forward: 5'-CTCTGCTGCCTCCTGGCTTCT-3'	Integrated DNA Technologies	Integrated DNA Technologies
Tom-GFP Wt Reverse: 5'-CGAGGCGGATCACAAGCAATA-3'	Integrated DNA Technologies	Integrated DNA Technologies
Tom-GFP Mut Reverse: 5'-TCAATGGGCGGGGTCGTT-3'	Integrated DNA Technologies	Integrated DNA Technologies
Prox1-CreER ^{T2} Forward: 5'-AACTCGAGCTCTTCTCTCTACAGTTCAACAGATGCATTACC-3'	Integrated DNA Technologies	Integrated DNA Technologies
Prox1-CreER ^{T2} Reverse: 5'-GGGGGAGGGAGAGGGGCGGAATTGCTACTCGTGAAGGAGTTC-3'	Integrated DNA Technologies	Integrated DNA Technologies

Supplementary Information The online version contains supplementary material available at <https://doi.org/10.1007/s10456-022-09831-y>.

Acknowledgements The authors thank Dr. Guillermo Oliver (Northwestern University) for providing the Prox1-CreER^{T2} mice and the members of the TTUHSC animal facility in Amarillo for their support. This work was supported in part by the National Institutes of Health Grant (NCI) R15CA231339 and Texas Tech University Health Sciences Center (TTUHSC) School of Pharmacy Office of the Sciences grant. The common equipment used was obtained through the Cancer Prevention Research Institute of Texas (CPRIT) Grants RP110786, RP190524 and RP200572. The funders had no role in study design, decision to write, or preparation of the manuscript.

Author contributions Conceptualization, RGA and CMM; Methodology, RGA, MSS; Validation, FTZ, CMM; Investigation, RGA, MSS, FTZ, MZM and CMM; Writing—Original Draft, RGA and CMM; Writing—Review & Editing, FTZ, MSS, PT, MZM, YZ, JSG and CLD; Resources, PT, YZ, JSG and CLD; Supervision, CMM; Funding Acquisition: CMM.

Declarations

Conflict of interest The authors declare no competing interests.

References

- Sato TN et al (1993) Tie-1 and tie-2 define another class of putative receptor tyrosine kinase genes expressed in early embryonic vascular system. *Proc Natl Acad Sci USA* 90(20):9355–9358
- Maisonpierre PC et al (1997) Angiopoietin-2, a natural antagonist for Tie2 that disrupts in vivo angiogenesis. *Science* 277(5322):55–60
- Akwii RG et al (2019) Role of angiopoietin-2 in vascular physiology and pathophysiology. *Cells* 8(5):471
- Tsigkos S, Koutsilieris M, Papapetropoulos A (2003) Angiopoietins in angiogenesis and beyond. *Expert Opin Investig Drugs* 12(6):933–941
- Davis S et al (1996) Isolation of angiopoietin-1, a ligand for the TIE2 receptor, by secretion-trap expression cloning. *Cell* 87(7):1161–1169
- Hansen TM et al (2010) Effects of angiopoietins-1 and -2 on the receptor tyrosine kinase Tie2 are differentially regulated at the endothelial cell surface. *Cell Signal* 22(3):527–532
- Teichert-Kuliszewska K et al (2001) Biological action of angiopoietin-2 in a fibrin matrix model of angiogenesis is associated with activation of Tie2. *Cardiovasc Res* 49(3):659–670
- Yuan HT et al (2009) Angiopoietin 2 is a partial agonist/antagonist of Tie2 signaling in the endothelium. *Mol Cell Biol* 29(8):2011–2022
- Kim I et al (2000) Angiopoietin-2 at high concentration can enhance endothelial cell survival through the phosphatidylinositol 3'-kinase/Akt signal transduction pathway. *Oncogene* 19(39):4549–4552
- Kim M et al (2016) Opposing actions of angiopoietin-2 on Tie2 signaling and FOXO1 activation. *J Clin Invest* 126(9):3511–3525
- Witzenbichler B et al (1998) Chemotactic properties of angiopoietin-1 and -2, ligands for the endothelial-specific receptor tyrosine kinase Tie2. *J Biol Chem* 273(29):18514–18521
- Mochizuki Y et al (2002) Angiopoietin 2 stimulates migration and tube-like structure formation of murine brain capillary endothelial cells through c-Fes and c-Fyn. *J Cell Sci* 115(Pt 1):175–183
- Nguyen VP et al (2007) Differential response of lymphatic, venous and arterial endothelial cells to angiopoietin-1 and angiopoietin-2. *BMC Cell Biol* 8:10
- Song SH et al (2012) Tie1 regulates the Tie2 agonistic role of angiopoietin-2 in human lymphatic endothelial cells. *Biochem Biophys Res Commun* 419(2):281–286
- Dumont DJ et al (1995) Vascularization of the mouse embryo: a study of flk-1, tek, tie, and vascular endothelial growth factor expression during development. *Dev Dyn* 203(1):80–92
- Partanen J, Dumont DJ (1999) Functions of Tie1 and Tie2 receptor tyrosine kinases in vascular development. *Curr Top Microbiol Immunol* 237:159–172
- Yamaguchi TP et al (1993) flk-1, an flt-related receptor tyrosine kinase is an early marker for endothelial cell precursors. *Development* 118(2):489–498
- Millauer B et al (1993) High affinity VEGF binding and developmental expression suggest Flk-1 as a major regulator of vasculogenesis and angiogenesis. *Cell* 72(6):835–846
- Kaipainen A et al (1993) The related FLT4, FLT1, and KDR receptor tyrosine kinases show distinct expression patterns in human fetal endothelial cells. *J Exp Med* 178(6):2077–2088
- Dumont DJ et al (1992) tek, a novel tyrosine kinase gene located on mouse chromosome 4, is expressed in endothelial cells and their presumptive precursors. *Oncogene* 7(8):1471–1480
- Dumont DJ et al (1993) The endothelial-specific receptor tyrosine kinase, tek, is a member of a new subfamily of receptors. *Oncogene* 8(5):1293–1301
- Dumont DJ et al (1994) Dominant-negative and targeted null mutations in the endothelial receptor tyrosine kinase, tek, reveal a critical role in vasculogenesis of the embryo. *Genes Dev* 8(16):1897–1909
- Morisada T et al (2005) Angiopoietin-1 promotes LYVE-1-positive lymphatic vessel formation. *Blood* 105(12):4649–4656
- Tammela T et al (2005) Angiopoietin-1 promotes lymphatic sprouting and hyperplasia. *Blood* 105(12):4642–4648
- Srinivasan RS et al (2007) Lineage tracing demonstrates the venous origin of the mammalian lymphatic vasculature. *Genes Dev* 21(19):2422–2432
- Pichol-Thievent C et al (2018) A blood capillary plexus-derived population of progenitor cells contributes to genesis of the dermal lymphatic vasculature during embryonic development. *Development*. <https://doi.org/10.1242/dev.160184>
- Mofarrah M, Hussain SN (2011) Expression and functional roles of angiopoietin-2 in skeletal muscles. *PLoS One* 6(7):e22882
- Koga K et al (2001) Expression of angiopoietin-2 in human glioma cells and its role for angiogenesis. *Cancer Res* 61(16):6248–6254
- Stratmann A, Risau W, Plate KH (1998) Cell type-specific expression of angiopoietin-1 and angiopoietin-2 suggests a role in glioblastoma angiogenesis. *Am J Pathol* 153(5):1459–1466
- Huang YQ et al (2002) Thrombin induces increased expression and secretion of angiopoietin-2 from human umbilical vein endothelial cells. *Blood* 99(5):1646–1650
- Gale NW et al (2002) Angiopoietin-2 is required for postnatal angiogenesis and lymphatic patterning, and only the latter role is rescued by Angiopoietin-1. *Dev Cell* 3(3):411–423
- Zhang L et al (2003) Tumor-derived vascular endothelial growth factor up-regulates angiopoietin-2 in host endothelium and destabilizes host vasculature, supporting angiogenesis in ovarian cancer. *Cancer Res* 63(12):3403–3412
- Hackett SF et al (2000) Angiopoietin 2 expression in the retina: upregulation during physiologic and pathologic neovascularization. *J Cell Physiol* 184(3):275–284
- Fiedler U et al (2004) The Tie-2 ligand angiopoietin-2 is stored in and rapidly released upon stimulation from endothelial cell Weibel–Palade bodies. *Blood* 103(11):4150–4156
- Daly C et al (2006) Angiopoietin-2 functions as an autocrine protective factor in stressed endothelial cells. *Proc Natl Acad Sci USA* 103(42):15491–15496
- Felcht M et al (2012) Angiopoietin-2 differentially regulates angiogenesis through TIE2 and integrin signaling. *J Clin Invest* 122(6):1991–2005
- Helaine C et al (2020) Angiopoietin-2 combined with radiochemotherapy impedes glioblastoma recurrence by acting in an autocrine and paracrine manner: a preclinical study. *Cancers (Basel)* 12(12):3585
- Lemieux C et al (2005) Angiopoietins can directly activate endothelial cells and neutrophils to promote proinflammatory responses. *Blood* 105(4):1523–1530
- Sfiligoi C et al (2003) Angiopoietin-2 expression in breast cancer correlates with lymph node invasion and short survival. *Int J Cancer* 103(4):466–474
- Kelly BD et al (2003) Cell type-specific regulation of angiogenic growth factor gene expression and induction of angiogenesis in nonischemic tissue by a constitutively active form of hypoxia-inducible factor 1. *Circ Res* 93(11):1074–1081
- Ridley AJ (2015) Rho GTPase signalling in cell migration. *Curr Opin Cell Biol* 36:103–112
- Mikelis CM et al (2013) PDZ-RhoGEF and LARG are essential for embryonic development and provide a link between thrombin and LPA receptors and Rho activation. *J Biol Chem* 288(17):12232–12243

43. Mikelis CM et al (2015) RhoA and ROCK mediate histamine-induced vascular leakage and anaphylactic shock. *Nat Commun* 6:6725
44. van Nieuw Amerongen GP et al (2003) Involvement of RhoA/Rho kinase signaling in VEGF-induced endothelial cell migration and angiogenesis in vitro. *Arterioscler Thromb Vasc Biol* 23(2):211–217
45. Zeng H, Zhao D, Mukhopadhyay D (2002) KDR stimulates endothelial cell migration through heterotrimeric G protein Gq/11-mediated activation of a small GTPase RhoA. *J Biol Chem* 277(48):46791–46798
46. Bryan BA et al (2010) RhoA/ROCK signaling is essential for multiple aspects of VEGF-mediated angiogenesis. *Faseb J* 24(9):3186–3195
47. Zahra FT et al (2019) Endothelial RhoA GTPase is essential for in vitro endothelial functions but dispensable for physiological in vivo angiogenesis. *Sci Rep* 9(1):11666
48. Sainz-Jaspeado M, Claesson-Welsh L (2018) Cytokines regulating lymphangiogenesis. *Curr Opin Immunol* 53:58–63
49. Zheng W, Aspelund A, Alitalo K (2014) Lymphangiogenic factors, mechanisms, and applications. *J Clin Invest* 124(3):878–887
50. Coso S, Bovay E, Petrova TV (2014) Pressing the right buttons: signaling in lymphangiogenesis. *Blood* 123(17):2614–2624
51. Kumar B et al (2011) VEGF-C differentially regulates VEGF-A expression in ocular and cancer cells; promotes angiogenesis via RhoA mediated pathway. *Angiogenesis* 14(3):371–380
52. He M et al (2010) Vascular endothelial growth factor C promotes cervical cancer metastasis via up-regulation and activation of RhoA/ROCK-2/moesin cascade. *BMC Cancer* 10:170
53. Ganguly A et al (2012) Isolation of human umbilical vein endothelial cells and their use in the study of neutrophil transmigration under flow conditions. *J Vis Exp* 66:e4032
54. Fidler IJ (2003) The pathogenesis of cancer metastasis: the ‘seed and soil’ hypothesis revisited. *Nat Rev Cancer* 3(6):453–458
55. Shayan R, Achen MG, Stacker SA (2006) Lymphatic vessels in cancer metastasis: bridging the gaps. *Carcinogenesis* 27(9):1729–1738
56. Mellor RH et al (2010) Lymphatic dysfunction, not aplasia, underlies Milroy disease. *Microcirculation* 17(4):281–296
57. Connell F, Brice G, Mortimer P (2008) Phenotypic characterization of primary lymphedema. *Ann N Y Acad Sci* 1131:140–146
58. Croteau SE et al (2014) Kaposiform lymphangiomatosis: a distinct aggressive lymphatic anomaly. *J Pediatr* 164(2):383–388
59. Ji Y et al (2019) Kaposiform lymphangiomatosis and kaposiform hemangioendothelioma: similarities and differences. *Orphanet J Rare Dis* 14(1):165
60. Frye M et al (2020) EphrinB2-EphB4 signalling provides Rho-mediated homeostatic control of lymphatic endothelial cell junction integrity. *Elife*. <https://doi.org/10.7554/eLife.57732>
61. Norden PR et al (2020) Shear stimulation of FOXC1 and FOXC2 differentially regulates cytoskeletal activity during lymphatic valve maturation. *Elife*. <https://doi.org/10.7554/eLife.53814>
62. Crampton SP, Davis J, Hughes CC (2007) Isolation of human umbilical vein endothelial cells (HUVEC). *J Vis Exp* 3:183
63. Mikelis C et al (2009) Integrin alpha(v)beta(3) is a pleiotrophin receptor required for pleiotrophin-induced endothelial cell migration through receptor protein tyrosine phosphatase beta/zeta. *Faseb J* 23(5):1459–1469
64. Mikelis C et al (2011) A peptide corresponding to the C-terminal region of pleiotrophin inhibits angiogenesis in vivo and in vitro. *J Cell Biochem* 112(6):1532–1543
65. Melendez J et al (2011) RhoA GTPase is dispensable for actomyosin regulation but is essential for mitosis in primary mouse embryonic fibroblasts. *J Biol Chem* 286(17):15132–15137
66. Ren XD, Kiosses WB, Schwartz MA (1999) Regulation of the small GTP-binding protein Rho by cell adhesion and the cytoskeleton. *EMBO J* 18(3):578–585
67. Drummond RA et al (2018) GM-CSF therapy in human caspase recruitment domain-containing protein 9 deficiency. *J Allergy Clin Immunol* 142(4):1334–1338.e5
68. Srivastava S et al (2020) Low dose of penfluridol inhibits VEGF-induced angiogenesis. *Int J Mol Sci* 21(3):755
69. Hossian A et al (2018) Multipronged activity of combinatorial miR-143 and miR-506 inhibits Lung Cancer cell cycle progression and angiogenesis in vitro. *Sci Rep* 8(1):10495
70. Carpentier G, Martinelli M, Courty J, Cascone I (2012) Angiogenesis analyzer for ImageJ. In: 4th ImageJ user and developer conference proceedings. pp 198–201
71. Shevchenko A et al (2006) In-gel digestion for mass spectrometric characterization of proteins and proteomes. *Nat Protoc* 1(6):2856–2860
72. Akwii RG et al (2021) In vivo ear sponge lymphangiogenesis assay. *Methods Mol Biol* 2193:85–96
73. Garcia-Caballero M et al (2017) Modeling pre-metastatic lymphovascular niche in the mouse ear sponge assay. *Sci Rep* 7:41494
74. Durre T et al (2018) uPARAP/Endo180 receptor is a gatekeeper of VEGFR-2/VEGFR-3 heterodimerisation during pathological lymphangiogenesis. *Nat Commun* 9(1):5178
75. Luo J et al (2017) RhoA and RhoC are involved in stromal cell-derived factor-1-induced cell migration by regulating F-actin redistribution and assembly. *Mol Cell Biochem* 436(1–2):13–21
76. Kutys ML, Yamada KM (2014) An extracellular-matrix-specific GEF-GAP interaction regulates Rho GTPase crosstalk for 3D collagen migration. *Nat Cell Biol* 16(9):909–917
77. Wilde C et al (2000) Recognition of RhoA by *Clostridium botulinum* C3 exoenzyme. *J Biol Chem* 275(22):16478–16483
78. Toda A et al (2015) Rho GTPase recognition by C3 exoenzyme based on C3-RhoA complex structure. *J Biol Chem* 290(32):19423–19432
79. Wilde C, Vogelsgesang M, Aktories K (2003) Rho-specific *Bacillus cereus* ADP-ribosyltransferase C3 cloning and characterization. *Biochemistry* 42(32):9694–9702
80. Kim KL et al (2006) Interaction between Tie receptors modulates angiogenic activity of angiopoietin2 in endothelial progenitor cells. *Cardiovasc Res* 72(3):394–402
81. Korhonen EA et al (2016) Tie1 controls angiopoietin function in vascular remodeling and inflammation. *J Clin Invest* 126(9):3495–3510
82. Hakanpaa L et al (2015) Endothelial destabilization by angiopoietin-2 via integrin beta1 activation. *Nat Commun* 6:5962
83. Huttenlocher A, Horwitz AR (2011) Integrins in cell migration. *Cold Spring Harb Perspect Biol* 3(9):a005074
84. Zhao X, Guan JL (2011) Focal adhesion kinase and its signaling pathways in cell migration and angiogenesis. *Adv Drug Deliv Rev* 63(8):610–615
85. Golubovskaya VM et al (2008) A small molecule inhibitor, 1,2,4,5-benzenetetraamine tetrahydrochloride, targeting the y397 site of focal adhesion kinase decreases tumor growth. *J Med Chem* 51(23):7405–7416
86. Brandvold KR et al (2012) Development of a highly selective c-Src kinase inhibitor. *ACS Chem Biol* 7(8):1393–1398
87. Jaffe AB, Hall A (2005) Rho GTPases: biochemistry and biology. *Annu Rev Cell Dev Biol* 21:247–269
88. Guilluy C et al (2011) The Rho GEFs LARG and GEF-H1 regulate the mechanical response to force on integrins. *Nat Cell Biol* 13(6):722–727
89. Patel M, Karginov AV (2014) Phosphorylation-mediated regulation of GEFs for RhoA. *Cell Adh Migr* 8(1):11–18

90. Matsui T et al (1996) Rho-associated kinase, a novel serine/threonine kinase, as a putative target for small GTP binding protein Rho. *Embo J* 15(9):2208–2216
91. Gavard J, Patel V, Gutkind JS (2008) Angiopoietin-1 prevents VEGF-induced endothelial permeability by sequestering Src through mDia. *Dev Cell* 14(1):25–36
92. Kalappurakkal JM et al (2019) Integrin mechano-chemical signaling generates plasma membrane nanodomains that promote cell spreading. *Cell* 177(7):1738–1756.e23
93. Breitsprecher D, Goode BL (2013) Formins at a glance. *J Cell Sci* 126(Pt 1):1–7
94. Kuhn S, Geyer M (2014) Formins as effector proteins of Rho GTPases. *Small GTPases* 5:e29513
95. Takeya R et al (2008) The mammalian formin FHOD1 is activated through phosphorylation by ROCK and mediates thrombin-induced stress fibre formation in endothelial cells. *Embo J* 27(4):618–628
96. Muzumdar MD et al (2007) A global double-fluorescent Cre reporter mouse. *Genesis* 45(9):593–605
97. Basu S, Kustanovich I, Lamprecht R (2016) Arp2/3 and VASP are essential for fear memory formation in lateral amygdala. *eNeuro*. <https://doi.org/10.1523/ENEURO.0302-16.2016>
98. Silveira AAA et al (2018) TNF induces neutrophil adhesion via formin-dependent cytoskeletal reorganization and activation of beta-integrin function. *J Leukoc Biol* 103(1):87–98
99. Scholz A, Plate KH, Reiss Y (2015) Angiopoietin-2: a multifaceted cytokine that functions in both angiogenesis and inflammation. *Ann N Y Acad Sci* 1347:45–51
100. Holopainen T et al (2012) Effects of angiopoietin-2-blocking antibody on endothelial cell-cell junctions and lung metastasis. *J Natl Cancer Inst* 104(6):461–475
101. Lewis CE, Ferrara N (2011) Multiple effects of angiopoietin-2 blockade on tumors. *Cancer Cell* 19(4):431–433
102. Mazziari R et al (2011) Targeting the ANG2/TIE2 axis inhibits tumor growth and metastasis by impairing angiogenesis and disabling rebounds of proangiogenic myeloid cells. *Cancer Cell* 19(4):512–526
103. Goede V et al (2010) Identification of serum angiopoietin-2 as a biomarker for clinical outcome of colorectal cancer patients treated with bevacizumab-containing therapy. *Br J Cancer* 103(9):1407–1414
104. Zonneveld R et al (2017) Low serum angiopoietin-1, high serum angiopoietin-2, and high Ang-2/Ang-1 protein ratio are associated with early onset sepsis in surinamese newborns. *Shock* 48(6):638–643
105. Michalska-Jakubus M et al (2019) Imbalanced serum levels of Ang1, Ang2 and VEGF in systemic sclerosis: integrated effects on microvascular reactivity. *Microvasc Res* 125:103881
106. Li P et al (2015) Diagnostic and prognostic potential of serum angiopoietin-2 expression in human breast cancer. *Int J Clin Exp Pathol* 8(1):660–664
107. Boureux A et al (2007) Evolution of the Rho family of ras-like GTPases in eukaryotes. *Mol Biol Evol* 24(1):203–216
108. Ridley AJ, Hall A (1992) The small GTP-binding protein rho regulates the assembly of focal adhesions and actin stress fibers in response to growth factors. *Cell* 70(3):389–399
109. Spindler V, Schlegel N, Waschke J (2010) Role of GTPases in control of microvascular permeability. *Cardiovasc Res* 87(2):243–253
110. Cascone I et al (2003) Tie-2-dependent activation of RhoA and Rac1 participates in endothelial cell motility triggered by angiopoietin-1. *Blood* 102(7):2482–2490
111. Mammoto T et al (2007) Angiopoietin-1 requires p190 RhoGAP to protect against vascular leakage in vivo. *J Biol Chem* 282(33):23910–23918
112. Souma T et al (2018) Context-dependent functions of angiopoietin 2 are determined by the endothelial phosphatase VEPTP. *Proc Natl Acad Sci USA* 115(6):1298–1303
113. Hynes RO (2002) Integrins: bidirectional, allosteric signaling machines. *Cell* 110(6):673–687
114. Danilucci TM et al (2019) Recombinant RGD-disintegrin DisBa-01 blocks integrin alphavbeta3 and impairs VEGF signaling in endothelial cells. *Cell Commun Signal* 17(1):27
115. Takada YK et al (2017) Direct binding to integrins and loss of disulfide linkage in interleukin-1beta (IL-1beta) are involved in the agonistic action of IL-1beta. *J Biol Chem* 292(49):20067–20075
116. Hu B et al (2006) Angiopoietin 2 induces glioma cell invasion by stimulating matrix metalloproteinase 2 expression through the alphavbeta1 integrin and focal adhesion kinase signaling pathway. *Cancer Res* 66(2):775–783
117. Imanishi Y et al (2007) Angiopoietin-2 stimulates breast cancer metastasis through the alpha(5)beta(1) integrin-mediated pathway. *Cancer Res* 67(9):4254–4263
118. Bezuidenhout L, Zilla P, Davies N (2009) Association of Ang-2 with integrin beta 2 controls Ang-2/PDGF-BB-dependent upregulation of human peripheral blood monocyte fibrinolysis. *Inflammation* 32(6):393–401
119. Thomas M et al (2010) Angiopoietin-2 stimulation of endothelial cells induces alphavbeta3 integrin internalization and degradation. *J Biol Chem* 285(31):23842–23849
120. Ruoslahti E (1996) RGD and other recognition sequences for integrins. *Annu Rev Cell Dev Biol* 12:697–715
121. Schmidt A, Hall A (2002) Guanine nucleotide exchange factors for Rho GTPases: turning on the switch. *Genes Dev* 16(13):1587–1609
122. Iwanicki MP et al (2008) FAK, PDZ-RhoGEF and ROCKII cooperate to regulate adhesion movement and trailing-edge retraction in fibroblasts. *J Cell Sci* 121(Pt 6):895–905
123. Lauffenburger DA, Horwitz AF (1996) Cell migration: a physically integrated molecular process. *Cell* 84(3):359–369
124. Higgs HN (2005) Formin proteins: a domain-based approach. *Trends Biochem Sci* 30(6):342–353
125. Courtemanche N (2018) Mechanisms of formin-mediated actin assembly and dynamics. *Biophys Rev* 10(6):1553–1569
126. Alberts AS et al (1998) Analysis of RhoA-binding proteins reveals an interaction domain conserved in heterotrimeric G protein beta subunits and the yeast response regulator protein Skn7. *J Biol Chem* 273(15):8616–8622
127. Scharpfenecker M et al (2005) The Tie-2 ligand angiopoietin-2 destabilizes quiescent endothelium through an internal autocrine loop mechanism. *J Cell Sci* 118(Pt 4):771–780
128. Brash JT et al (2020) Tamoxifen-activated CreERT impairs retinal angiogenesis independently of gene deletion. *Circ Res* 127(6):849–850
129. Jafree DJ et al (2021) Mechanisms and cell lineages in lymphatic vascular development. *Angiogenesis* 24(2):271–288
130. Geng X et al (2020) S1PR1 regulates the quiescence of lymphatic vessels by inhibiting laminar shear stress-dependent VEGF-C signaling. *JCI Insight*. <https://doi.org/10.1172/jci.insight.137652>

Publisher's Note Springer Nature remains neutral with regard to jurisdictional claims in published maps and institutional affiliations.